

# Pretaporter, a Drosophila protein serving as a ligand for Draper in the phagocytosis of apoptotic cells

メタデータ	言語: eng 出版者: 公開日: 2017-10-04 キーワード (Ja): キーワード (En): 作成者: メールアドレス: 所属:
URL	<a href="https://doi.org/10.24517/00015277">https://doi.org/10.24517/00015277</a>

This work is licensed under a Creative Commons Attribution-NonCommercial-ShareAlike 3.0 International License.



# **Pretaporter, a *Drosophila* protein serving as a ligand for Draper in the phagocytosis of apoptotic cells**

Running title: Pretaporter as Draper ligand

Takayuki Kuraishi,<sup>1,7</sup> Yukiko Nakagawa,<sup>2</sup> Kaz Nagaosa,<sup>2</sup> Yumi Hashimoto,<sup>1</sup> Takashi Ishimoto,<sup>2</sup> Takeshi Moki,<sup>2</sup> Yu Fujita,<sup>1</sup> Hiroshi Nakayama,<sup>4</sup> Naoshi Dohmae,<sup>4</sup> Akiko Shiratsuchi,<sup>1,2,3</sup> Naoko Yamamoto,<sup>2</sup> Koichi Ueda,<sup>3</sup> Masamitsu Yamaguchi,<sup>5</sup> Takeshi Awasaki<sup>6</sup> and Yoshinobu Nakanishi<sup>1,2,3,\*</sup>

<sup>1</sup>Graduate School of Medical Science, Kanazawa University, Kanazawa, Ishikawa 920-1192, Japan

<sup>2</sup>Graduate School of Natural Science and Technology, Kanazawa University, Kanazawa, Ishikawa 920-1192, Japan

<sup>3</sup>Faculty of Pharmaceutical Sciences, Kanazawa University, Kanazawa, Ishikawa 920-1192, Japan

<sup>4</sup>Biomolecule Characterization Team, RIKEN, Wako, Saitama 351-0198, Japan

<sup>5</sup>Department of Applied Biology, Kyoto Institute of Technology, Kyoto, Kyoto 606-8585, Japan

<sup>6</sup>Department of Neurobiology, University of Massachusetts Medical School, Worcester, MA 01605, USA

<sup>7</sup>Present address: Global Health Institute, EPFL, CH-1015 Lausanne, Switzerland

\*Corresponding author. Graduate School of Medical Science, Kanazawa University, Shizenken, Kakuma-machi, Kanazawa, Ishikawa 920-1192, Japan. Phone: +81 76 234 4481; Fax: +81 76 234 4480; E-mail: nakanaka@kenroku.kanazawa-u.ac.jp

Character count: 52,646

*Subject categories:* Development; Differentiation & Death

## Abstract

Phagocytic removal of cells undergoing apoptosis is necessary for animal development and tissue homeostasis. Draper, a homologue of the *Caenorhabditis elegans* phagocytosis receptor CED-1, is responsible for the phagocytosis of apoptotic cells in *Drosophila*, but its ligand presumably present on apoptotic cells remains unknown. An endoplasmic reticulum protein that binds to the extracellular region of Draper was isolated. Loss of this protein, which we name Pretaporter, led to a reduced level of apoptotic cell clearance in embryos, and the overexpression of *pretaporter* in the mutant flies rescued this defect. Results from genetic analyses suggested that Pretaporter functionally interacts with Draper and the corresponding signal mediators. Pretaporter was exposed at the cell surface after the induction of apoptosis, and cells artificially expressing Pretaporter at their surface became susceptible to Draper-mediated phagocytosis. Finally, the incubation with Pretaporter augmented the tyrosine-phosphorylation of Draper in phagocytic cells. These results collectively suggest that Pretaporter relocates from the endoplasmic reticulum to the cell surface during apoptosis to serve as a ligand for Draper in the phagocytosis of apoptotic cells.

*Keywords:* apoptosis / *Drosophila* / endoplasmic reticulum / phagocytosis

## Introduction

Throughout the life of multi-cellular organisms, cells of particular types die and are eventually eliminated in certain places in the body and at certain developmental stages under physiological and sub-physiological conditions (Cohen, 1991; Cleveland, 1996; Jacobson *et al*, 1997; Vaux and Korsmeyer, 1999). Such “unwanted cells” are mostly induced to undergo apoptosis and subjected to phagocytic elimination (Wyllie *et al*, 1980). Prompt and selective phagocytosis of apoptotic cells is prerequisite for morphogenesis, establishment of tissue functions, tissue renewal, avoidance of diseases, and effective progress of tissue functions (Savill and Fadok, 2000; Liao, 2005; Nakanishi *et al*, 2009).

There are two genetically identified signaling pathways that lead to the induction of phagocytosis of dying cells in *Caenorhabditis elegans* (Reddien and Horvitz, 2004; Kinchen and Hengartner, 2005; Mangahas and Zhou, 2005; Lettre and Hengartner, 2006): one is made up of the proteins CED-2, CED-5 and CED-12, and the other consists of CED-1, CED-6 and CED-7. The pathways converge at CED-10, a small G protein responsible for the rearrangement of cytoskeleton in phagocytes (Kinchen *et al*, 2005). The fact that all these *C. elegans* proteins possess counterparts in *Drosophila* and mammals (Lettre and Hengartner, 2006; Kinchen and Ravichandran, 2007) suggests that these two partially redundant signaling pathways are evolutionally conserved. However, the mode of action of those proteins still remains to be clarified, and there are missing components in the pathways. The selectivity in the recognition of apoptotic cells by phagocytes is due to the specific interaction between receptors of phagocytes and their ligands present at the surface of target cells (Lauber *et al*, 2004; Ravichandran and Lorenz, 2007). Presumably, there are two phagocytosis receptors in *C. elegans*, and CED-1 is likely the one located upstream of CED-6 and CED-7 (Zhou *et al*, 2001; Yu *et al*, 2006; Venegas and Zhou, 2007) while the other has not been found in genetic studies. Draper (Drpr), a *Drosophila* homologue of CED-1 (Callebaut *et al*, 2003), has been shown to act as a receptor in the phagocytosis of apoptotic cells (Freeman *et al*, 2003;

Manaka *et al*, 2004), and more recently molecules that act with Drpr to accomplish the engulfment and subsequent processing of apoptotic cells in *Drosophila* phagocytes were reported (Ziegenfuss *et al*, 2008; Kurant *et al*, 2008; Cuttell *et al*, 2008). However, a molecule(s) present at the surface of apoptotic cells and recognized by Drpr is yet to be identified. The study by Venegas and Zhou (2007) has implied that the membrane phospholipid phosphatidylserine, the best-characterized phagocytosis marker in mammals (Fadok *et al*, 1998; Schlegel and Williamson, 2001), could be a ligand for CED-1. In contrast, we showed that phosphatidylserine is not required in the Drpr-mediated phagocytosis of apoptotic cells (Manaka *et al*, 2004). In the present study, we searched for a phagocytosis marker(s) recognized by Drpr and identified an endoplasmic reticulum (ER) protein as a strong candidate.

## Results

### *Isolation of an ER protein that binds to the extracellular region of Drpr*

In search of a Drpr ligand(s), we adopted a biochemical approach to isolate a protein(s) that binds to Drpr. An extracellular portion of Drpr, which contained all 15 epidermal growth factor-like repeats (Callebaut *et al*, 2003), was prepared as a protein fused to glutathione *S*-transferase (GST) (Supplementary Figure S1A) using a vector derived from insect virus because Drpr likely undergoes a post-translational modification (Manaka *et al*, 2004). This protein, which we operationally named Drpr-GST, specifically bound to cycloheximide-treated S2 cells, a cell line established from *Drosophila* embryonic cells (Supplementary Figure S1B): treatment with cycloheximide makes S2 cells undergo typical apoptosis (see Figure 5) and susceptible to Drpr-mediated phagocytosis (Manaka *et al*, 2004). Drpr-GST was then covalently conjugated with glutathione-Sepharose, and whole-cell lysates of apoptotic S2 cells were chromatographed on this affinity matrix. The bound materials were eluted and analyzed by sodium dodecyl sulfate-polyacrylamide gel electrophoresis followed by staining with silver. The gel showed a band with a molecular mass of 47 kDa that was absent in the eluates from Sepharose containing GST alone (Figure 1A). A mass spectrometric analysis revealed that this protein, which we named Pretaporter (Prtp), encoded by the as-yet uncharacterized gene *CGI837* consists of 416 amino acid residues including the signal peptide at the amino terminus, three thioredoxin-like domains in the middle, and an ER retention motif at the carboxy terminus (Figure 1B). When the same eluates were analyzed by Western blotting with an antiserum raised against recombinant Prtp, a distinct signal was obtained at the expected position (Figure 1C). A cell-free binding assay using recombinant proteins revealed that two thirds of Prtp to the amino terminus is sufficient for the binding to Drpr-GST (Figure 1D). From these results, we concluded that Prtp is a *Drosophila* protein that binds to the extracellular region of Drpr.

We next determined the expression during development and the subcellular localization

of this newly identified protein. Prtp was expressed throughout the development of *Drosophila* as was Drpr (Figure 1E, and Supplementary Figure S2 for specificity of antibody) and in most cell types of embryos (Figure 1F) and wing discs (Figure 4C). A cytochemical analysis of dispersed embryonic cells showed that signals derived from Prtp overlapped with those of an ER marker (Figure 1G). These results indicated that Prtp is an ER protein expressed ubiquitously throughout development.

### ***Reduced level of apoptotic cell phagocytosis in prtp null mutants***

To assess a role for Prtp in the Drpr-mediated phagocytosis of apoptotic cells, we established fly lines deficient in its expression. A fly line that contains a P-element inserted proximal upstream of the translation start codon of *prtp* was subjected to P-element excision, and two mutations, *prtp*<sup>Δ1</sup> and *prtp*<sup>Δ2</sup>, which deleted a part of the first exon of *prtp*, were isolated (Figure 2A and Supplementary Figure S3A). We also obtained *prtp*<sup>G19</sup>, in which the P-element had been precisely excised. The expression of *prtp*, either mRNA or protein, was undetectable in homozygous mutants of both *prtp*<sup>Δ1</sup> and *prtp*<sup>Δ2</sup>, while *prtp*<sup>G19</sup> flies showed a normal level expression of *prtp* (Supplementary Figures S3B and S3C). The expression of *drpr* was not influenced in these three fly lines (Supplementary Figures S3B and S3C). These results indicated that two null alleles of *prtp*, *prtp*<sup>Δ1</sup> and *prtp*<sup>Δ2</sup>, were generated. The fly line *prtp*<sup>G19</sup> was used thereafter as a control in the analysis of the mutant alleles. Either mutant fly line was viable as a homozygote, and there was no defect in their development, motility, or fertility (data not shown). We first examined whether or not a loss of *prtp* expression influences the occurrence of apoptosis during embryogenesis, which becomes apparent at the developmental stage 11 (Abrams *et al*, 1993). Whole embryos at stages 10 and 11 were subjected to immunohistochemistry with anti-activated caspase-3 antibody as well as terminal deoxynucleotidyltransferase-mediated dUTP nick end labeling (TUNEL) for the analysis of caspase activation and DNA fragmentation, respectively. Cells containing activated caspase or fragmented DNA were absent at stage 10 and became detectable around the anterior part

of embryos at stage 11 of the control flies, and this was almost the same for the mutant flies (Supplementary Figure S4). These results indicated that apoptosis occurs normally in embryos lacking Prtp. We then determined the level of phagocytosis of apoptotic cells by hemocytes and glia in embryos, which we previously reported to accomplish Drpr-mediated phagocytosis (Manaka *et al*, 2004).

Hemocytes, which were labeled with green fluorescent protein (GFP) using a specific promoter, were widely distributed in embryos as reported previously (Brückner *et al*, 2004), and the distribution (left panel in Figure 2B) and population (right panel in Figure 2B) of hemocytes in embryos remained the same irrespective of the expression of *prtp*. When those embryos were subjected to TUNEL, some of the GFP-positive hemocytes contained positively stained nuclei besides their own (left panel in Figure 2C). We thus counted the cells positive for both GFP and TUNEL as those hemocytes that had phagocytosed apoptotic cells, and determined the ratio of phagocytosing hemocytes. Only hemocytes residing near the peripheral part of embryos were analyzed because individual hemocytes were hardly discriminated in the middle part. The results showed that the level of phagocytosis in either *prtp*<sup>Δ1</sup> or *prtp*<sup>Δ2</sup> was almost half of that in the control *prtp*<sup>G19</sup> (right panel in Figure 2C) (note that the level of phagocytosis in *prtp*<sup>G19</sup> was equivalent to that in the fly line *w*<sup>1118</sup>). In order to investigate hemocytes including those residing in other parts of embryos, embryos were mechanically disrupted, and resulting dispersed cells were analyzed. As were observed with intact embryos, GFP-positive hemocytes with and without TUNEL-stained nuclei were present in the dispersed cells, and the ratio of phagocytosing hemocytes was significantly lower in the mutant embryos than in the control (Figure 2D). To confirm the importance of Prtp, we examined whether the overexpression of *prtp* in the mutants rescues the phagocytosis phenotype. In this experiment, embryonic hemocytes were identified by immunohistochemically examining the presence of Croquemort, a marker for hemocytes (Franc *et al*, 1996; 1999) (Supplementary Figure S5). The defect in phagocytosis in *prtp*<sup>Δ1</sup> was completely recovered by the ubiquitous expression of *prtp* using the *daughterless* (*da*) promoter (Figure 2E),

indicating that Prtp indeed plays a role in the phagocytosis of apoptotic cells. In contrast, the expression of *prtp* in a hemocyte-specific manner using the *serpent* (*srp*) promoter did not alter the level of phagocytosis (Figure 2E), suggesting that Prtp is required in apoptotic cells not hemocytes. In fact, the level of the phagocytosis of latex beads, indicative of the basal phagocytic activity of phagocytes, was the same between larval hemocytes isolated from the control and *prtp* mutant flies (Figure 2F).

We next examined the phagocytosis of apoptotic cells by glia in the *prtp* mutants. The distribution (left panel in Figure 2G) and number (right panel in Figure 2G) of glia, which were immunohistochemically visualized with antibody recognizing the glia-specific protein Repo, did not significantly differ in embryos between the control and *prtp* mutants. To determine the level of phagocytosis *in situ*, *Rep1<sup>P</sup>*, a null allele of *dICAD* (Mukae *et al*, 2002), was introduced into *prtp<sup>Δ1</sup>*, *prtp<sup>Δ2</sup>* and *prtp<sup>G19</sup>*. In *Rep1<sup>P</sup>* flies, the active form of caspase-activated DNase is not produced and, thus, DNA of apoptotic cells is degraded only after engulfment by phagocytes (Mukae *et al*, 2002). We previously showed that apoptotic cells engulfed by phagocytes in these flies are detectable by *in situ* nick translation (ISNT) (Manaka *et al*, 2004). The region in the ventral nerve cord of stage 16 embryos contains many glia that phagocytose apoptotic neurons (Abrams *et al*, 1993; Sonnenfeld and Jacobs, 1995). We therefore determined the number of ISNT signals detected in the nine abdominal segments (A1 to A9) of the ventral nerve cord in stage 16 embryos (see left panel in Figure 2G). The level of phagocytosis in the *prtp* mutants was about a half of that observed in control embryos (Figure 2H). To further confirm a defect in the phagocytosis of apoptotic cells by glia in the *prtp* mutants, dispersed embryonic cells were analyzed for the level of phagocytosis as done for the analysis of phagocytosis by hemocytes, except for the use of the glial marker Repo instead of Croquemort (left panel in Figure 2I). We found that the level of Repo-positive glia that contained TUNEL-positive nuclei was reduced in the *prtp* mutants (right panel in Figure 2I).

Furthermore, when *prtp* was overexpressed in *Rep1<sup>P</sup>* flies that normally express *prtp*, the level of apoptotic cell phagocytosis in embryos increased and the number of apoptotic cells

decreased (Supplementary Figure S6). All these results indicated that Prtp is required for the efficient phagocytosis of apoptotic cells by hemocytes and glia in *Drosophila* embryos. We previously reported that Drpr is responsible for the phagocytic removal of degenerated axons in mushroom body  $\gamma$  neurons by glia during metamorphosis (Awasaki *et al*, 2006). However, the timing and extent of the loss of the axons were the same between the control and *prtp* mutant (Supplementary Figure S7).

### **Genetic interaction of *prtp* with *drpr*, *ced-6*, and *Rac1/Rac2***

Ced-6, a *Drosophila* homologue of *C. elegans* CED-6, plays a role in the Drpr-mediated phagocytosis of neural axons by glia (Awasaki *et al*, 2006). More recently, Franc and co-workers reported that *drpr* genetically interacts with *ced-6* with regard to the phagocytosis of apoptotic cells (Cuttell *et al*, 2008). An immunohistochemical analysis showed that most embryonic hemocytes expressed Ced-6 (Supplementary Figure S8A). We thus genetically examined whether or not Prtp functions in the pathway where Drpr and Ced-6 are involved. To obtain a null allele of *ced-6*, we generated a fly line having a deletion in the region spanning *ced-6* by P-element excision (Supplementary Figure S8B). This mutant, *ced-6<sup>J26</sup>*, lacked the expression of Ced-6 with no change in the expression of Drpr and Prtp (Supplementary Figure S8C). We found that embryonic hemocytes of this *ced-6* null mutant showed a lower level of phagocytosis than those of wild-type flies (Figure 3A), confirming the involvement of Ced-6 in the phagocytosis of apoptotic cells (Cuttell *et al*, 2008). We then examined phagocytosis in the *prtp* null mutant with additional mutation on *drpr* (*drpr<sup>A5</sup>*, see Supplementary Figure S2C) or *ced-6*, but the loss of either Drpr or Ced-6 did not further decrease the level of phagocytosis (Figure 3A), suggesting that Prtp and Drpr, and Prtp and Ced-6 act in the same pathway. We next examined the occurrence of genetic interaction between *prtp* and *drpr*, and *prtp* and *ced-6*. A heterozygous mutant for each of the three genes, which had reduced expression of the corresponding proteins (top panel of Figure 3B), showed a level of phagocytosis comparable to that observed with control *w<sup>1118</sup>* flies (bottom panel

of Figure 3B). However, the level of phagocytosis by embryonic hemocytes of a *trans*-heterozygous mutant for *prtp* and either *drpr* or *ced-6* was significantly lower than that by hemocytes of the control flies (bottom panel of Figure 3B). These results indicated that *prtp* genetically interacts with *drpr* and *ced-6*. Taken together, Prtp, Drpr, and Ced-6 are likely to function in the same signaling pathway for the induction of phagocytosis of apoptotic cells.

We extended genetic studies to examine the possible interaction of *prtp* with other *Drosophila* genes homologous to those consisting of the engulfment pathways in *C. elegans*. An analysis of genetic interaction for *mbc* (*CED-5* homologue) and *Rac1* and *Rac2* (*CED-10* homologues) was carried out because null mutants for *mbc* (Nolan *et al*, 1998) and both *Rac1* and *Rac2* (Hakeda-Suzuki *et al*, 2002) show developmental defects in embryos. We found that embryos of *trans*-heterozygotes of *prtp*<sup>Δ1</sup> and *mbc*<sup>Cl</sup> (null mutant of *mbc*) showed the level of phagocytosis by hemocytes comparable to that with a heterozygous mutant for each gene (Figure 3C). In contrast, the level of phagocytosis in embryos lacking one copy of *prtp*, *Rac1*, and *Rac2* was lower than that in a heterozygous mutant for *prtp*, or *Rac1* and *Rac2* (Figure 3C), further suggesting the involvement of Prtp in the pathway corresponding to CED-1/CED-6/CED-10 in *C. elegans*. To our surprise, a lack of the expression of *elmo* (*CED-12* homologue) did not seem to affect phagocytosis in embryos (Figure 3D), indicating that ELMO does not play an important role in the phagocytosis of apoptotic cells in embryos. We were unable to analyze a *Drosophila* gene homologous to *CED-2* because of a technical difficulty. These results collectively suggested that Prtp is not involved in the engulfment pathway corresponding to CED-2/CED-5/CED-12 in *C. elegans*.

We previously reported that Calreticulin, another protein residing in the ER, serves as a marker for phagocytosis in *Drosophila* embryos (Kuraishi *et al*, 2007). We thus genetically examined the relationship between *prtp* and *calreticulin* as to the phagocytosis of apoptotic cells. When cells dispersed from embryos were analyzed, the ratio of phagocytosing hemocytes obtained from a double mutant for *prtp* and *calreticulin* was about 70% of that from the *prtp* single mutant

(Supplementary Figure S9A). Furthermore, the level of phagocytosis in embryos of *trans*-heterozygotes of *prtp*<sup>Δ1</sup> and a *calreticulin* null allele was almost the same as that in embryos of flies lacking one copy of *prtp* or *calreticulin* (Supplementary Figure S9B), suggesting that there was no genetic interaction between these two genes. Taken together, it seems likely that Prtp and Calreticulin play independent roles in the phagocytosis of apoptotic cells by embryonic hemocytes.

### ***Relocation of Prtp to the cell surface during apoptosis***

We next examined a possible change in the subcellular localization of Prtp during apoptosis. S2 cells before and after the induction of apoptosis by the treatment with cycloheximide were examined by immunocytochemistry under conditions without membrane permeabilization. We found that the occurrence of apoptosis rendered S2 cells positive for the surface expression of Prtp (Figure 4A). To confirm this *in vivo*, cells dispersed from embryos, in which apoptosis was induced by the overexpression of Reaper and Hid, were analyzed for the externalization of Prtp. Most dispersed embryonic cells with externalized phosphatidylserine, indicative of apoptosis, were also positive for the binding of anti-Prtp antibody (Figure 4B). We then extended this type of analysis using wing discs where only a few cells undergo apoptosis in normal development (Milán *et al*, 1997). Spatio- and temporal-specific apoptosis was induced in the discs by the expression of *reaper* and *hid* under the *engrailed* promoter, and these discs were analyzed for externalized Prtp (Figure 4C). Apoptosis examined by ISNT was evident in a portion of the disc where the *engrailed* promoter is presumed to be active (Tabata *et al*, 1995), and the same region simultaneously became positive for the surface expression of Prtp (first row): note that most Prtp-positive cells were also positive for the ISNT signal. Positive staining with anti-Prtp antibody was not due to the permeabilization of plasma membranes, because antibody that recognizes tubulin did not bind to the region of apoptosis unless the discs were membrane permeabilized (second and fourth rows). In addition, ubiquitous expression of Prtp was observed after the permeabilization of membranes (third row). These results indicated that apoptosis causes the exposure of Prtp at the

cell surface. We next determined the timing of Prtp externalization during apoptosis using S2 cells. The data suggested that the externalization of Prtp occurs at almost the same time as the fragmentation of DNA, and after the loss of phospholipid asymmetry in the plasma membrane and the cleavage of pro-caspase-3 (Figure 5A). Furthermore, the surface expression of Prtp in S2 cells was not observed when caspases were inhibited during the induction of apoptosis (Figure 5B). Taken together, these results show that Prtp relocates from the ER to the cell surface during the process of apoptosis.

### ***Role of Prtp as a ligand for Drpr in the phagocytosis of apoptotic cells***

The results obtained so far suggested that Prtp acts as a ligand for Draper in the phagocytosis of apoptotic cells. In order to obtain data more directly supporting this idea, we carried out a series of experiments. First, we asked if the surface expression of Prtp makes particles more effective targets for phagocytosis. Recombinant Prtp fused to GST was covalently attached to latex beads, and these particles were tested as targets for l(2)mbn cells, a *Drosophila* cell line derived from larval hemocytes, which acquire the ability to phagocytose apoptotic S2 cells in a Drpr-dependent manner after the treatment with 20-hydroxyecdysone (Manaka *et al*, 2004). We found that Prtp-coated latex beads were more efficiently phagocytosed by hormone-treated l(2)mbn cells than those coated with GST alone (Figure 6A). Furthermore, the enhancement of phagocytosis by Prtp was completely suppressed when Drpr expression in l(2)mbn cells was inhibited by RNA interference. This indicated that the presence of Prtp at the surface of target particles renders Drpr-mediated phagocytosis more effective. We next confirmed this observation using cells instead of artificial targets. To make the ER protein Prtp expressed at the cell surface, cDNA was manipulated so that the ER retention motif of Prtp was replaced with an amino acid sequence for the attachment of the glycosylphosphatidylinositol anchor (Supplementary Figure S10A). S2 cells transfected with this DNA became positive for the surface exposure of Prtp (left panel of Figure 6B) and were more efficiently phagocytosed by hormone-treated l(2)mbn cells than those transfected

with the vector alone or left untransfected (right panel of Figure 6B). This enhancement seemed Drpr dependent because RNA interference-mediated inhibition of Drpr expression in l(2)mbn cells reduced phagocytosis (Supplementary Figure S10B). Drpr is presumed to undergo tyrosine phosphorylation at the intracellular region upon activation (Mangahas and Zhou, 2005; Ziegenfuss *et al*, 2008). We thus next tested if the binding of Prtp induces the phosphorylation of Drpr. To do so, l(2)mbn cells were maintained in culture containers coated with recombinant Prtp, and their whole-cell lysates were subjected to immunoprecipitation with anti-Drpr antibody followed by Western blotting with anti-phosphotyrosine antibody. The results showed that the amount of tyrosine-phosphorylated Drpr in l(2)mbn cells increased after incubation with Prtp, but not with a control protein (Figure 6C). All the data described above collectively strengthened the idea that Prtp serves as a ligand for Drpr in the phagocytosis of apoptotic cells.

## Discussion

Here, we report the identification of a *Drosophila* protein, which we have named Prtp, serving as a ligand for Drpr in the phagocytosis of apoptotic cells. The level of phagocytosis in embryos of the null mutants for *prtp* and *drpr* was almost the same and about half of that in controls. This suggests that Prtp is solely responsible for the Drpr-mediated phagocytosis by embryonic hemocytes, and that there are additional ligands and receptors for phagocytosis. **Based on the data presented above, we would propose the following pathway for the induction of the Prtp-dependent, Drpr-mediated phagocytosis of apoptotic cells: Prtp relocates from the ER to the cell surface during apoptosis; Prtp binds to Drpr of hemocytes and induces tyrosine phosphorylation; Ced-6 binds to phosphorylated Drpr and further transmits the signal leading to the activation of Rac1 and/or Rac2; and cytoskeletons are reorganized for engulfment.** Additional molecules could participate in this pathway: a membrane protein named Six-microns-under reportedly acts upstream of Drpr in the phagocytosis of apoptotic neurons by glia (Kurant *et al*, 2008); another signal mediator, named Shark, located proximal downstream of Drpr has been reported (Ziegenfuss *et al*, 2008); and Undertaker, an intracellular membrane protein involved in the regulation of calcium homeostasis, was shown to function downstream of Drpr (Cuttell *et al*, 2008). In particular, Six-microns-under has been suggested to bridge glia and apoptotic neurons (Kurant *et al*, 2008). Our results suggested that Prtp still serves as a ligand for Drpr in the phagocytosis by glia that express Six-microns-under. Further investigation is necessary before we obtain a complete picture of the Prtp/Drpr-initiated signaling pathway for the phagocytosis of apoptotic cells. More molecules are involved in the phagocytosis of apoptotic cells in *Drosophila*: the receptor Croquemort (Franc *et al*, 1996; 1999), the phagocytosis marker Calreticulin (Kuraishi *et al*, 2007), and Pallbearer, a component of ubiquitin ligase (Silva *et al*, 2007), which might be integrated into the other engulfment pathway.

Prtp normally resides in the ER, most likely in its lumen, and a portion of it seems to

relocate to the cell surface during apoptosis. The ER and plasma membranes exchange their components (Levine and Rabouille, 2005), and this might be enhanced upon the induction of apoptosis. In fact, Herrmann and co-workers reported that a variety of proteins and lipids of the ER are exposed at the surface of apoptotic human cells (Franz *et al*, 2007). More recently, it was reported that the exposure of ER proteins at the surface of apoptotic mammalian cells occurs by SNARE-dependent exocytosis (Panaretakis *et al*, 2009). It is thus probable that together with other ER components Prtp moves to the cell surface during apoptosis and serves as a ligand for the phagocytosis receptor Drpr. Prtp seemed dispensable for the removal of degenerated neural axons during metamorphosis, which requires the action of Drpr (Awasaki *et al*, 2006). We speculate that Prtp is not exposed on the surface of degenerated axons because the removal of these axons occurs independently of caspases (Awasaki *et al*, 2006), and that another ligand for Drpr exists at the surface of degenerated axons. On the other hand, Drpr appears to serve as a receptor in the phagocytosis of bacteria (Cuttell *et al*, 2008; Hashimoto *et al*, 2009). Taken together, it is likely that Drpr is a multi-ligand receptor for phagocytosis responsible for the maintenance of tissue homeostasis through the removal of degenerated own cells and invading microbial pathogens.

A counterpart for Prtp in *C. elegans* could be a ligand for CED-1, but there seems no complete homologue of *prtp* in its genome. Our data suggested that the presence of two thioredoxin-like domains is sufficient for the binding of Prtp to Drpr. Therefore, a *C. elegans* protein containing such a structure, PDI for example, is a candidate for the CED-1 ligand. In contrast, the mammalian homologue of Prtp seems to exist; a mouse protein called ERp46 (Knoblach *et al*, 2003) and human proteins belonging to the TXNDC5 family (Nissom *et al*, 2006) possess a domain composition similar to that of Prtp. It is important to examine if *C. elegans* PDI and mammalian ERp46 and TXNDC5 act as ligands for CED-1 and its mammalian homologue MEGF10 (Hamon *et al*, 2006), respectively, in the phagocytosis of apoptotic cells.

## Materials and methods

### *Fly stocks and cell culture*

The following fly lines were used in this study:  $w^{1118}$ ,  $CG1837^{BG00450}$  (Bloomington Drosophila Stock Center),  $ced-6^{EY11592}$  (Bloomington Drosophila Stock Center),  $P\{seq-EYFP-ER\}3$  (LaJeunesse *et al*, 2004),  $RepI^p$  (Mukae *et al*, 2002),  $srpHemo-GAL4$   $UAS-srcEGFP$  (Brückner *et al*, 2004),  $en-GAL4$  (Brand and Perrimon, 1993),  $da-GAL4$  (Giebel *et al*, 1997),  $tub-GAL80^{ts20}$  (McGuire *et al*, 2003),  $UAS-cGFP$   $S65T$  (a gift from B Dickson),  $UAS-rpr$   $UAS-hid$  (Zhou *et al*, 1997),  $drpr^{\Delta 5}$  (Freeman *et al*, 2003; MacDonald *et al*, 2006),  $201Y-GAL4$  (Yang *et al*, 1995),  $mbc^{Cl}$  (Rushton *et al*, 1995),  $elmo^{KO}$  (Bianco *et al*, 2007),  $Rac1^{J11}$  (Ng *et al*, 2002),  $Rac2^{\Delta}$  (Ng *et al*, 2002), and  $Crc^{S114307}$  (Prokopenko *et al*, 2000). In order to determine fly genotypes based on the expression of  $\beta$ -galactosidase,  $drpr^{\Delta 5}$ ,  $mbc^{Cl}$ , and  $Rac1^{J11}$   $Rac2^{\Delta}$  were balanced over TM3-*ftzlacZ*, and  $elmo^{KO}$  was balanced over CyO-*ftzlacZ*. The alleles of *prtp* analyzed were generated by imprecise excision of the P-element with  $CG1837^{BG00450}$ . After standard mitotic recombination over  $w^{1118}$  chromosomes to remove possible second-site mutations, the P-element was mobilized by a  $\Delta 2-3$  transposase source. About 200 candidate excision events were screened by genomic polymerase chain reaction amplifying the *prtp* locus (see Figure 2A and Supplementary Figure S3A), and two deletion lines,  $prtp^{\Delta 1}$  and  $prtp^{\Delta 2}$ , were isolated. A strain after precise excision of the P-element,  $prtp^{G19}$ , was also obtained and used as a control. A null allele for *ced-6*,  $ced-6^{J26}$ , was similarly generated by imprecise excision of the P-element with  $ced-6^{EY11592}$  (see Supplementary Figures S8B and S8C). To obtain flies containing an extra *prtp* expressed with the *GAL4-UAS* system, the entire coding region of Prtp cDNA isolated from the *Drosophila* EST clone LD24756 (provided by Berkeley Drosophila Genome Project and National Institute of Genetics) was inserted into pUAST (Brand and Perrimon, 1993), and flies transgenic with the resultant DNA were generated according to a standard procedure (Spradling, 1986; Robertson *et al*, 1988). Three fly lines carrying the transgene on the 2nd or 3rd chromosome were established, and one with it on

the 3rd chromosome was used for intercrossing with *da-GAL4* (for ubiquitous expression) or *srpHemo-GAL4 UAS-srcEGFP* (for hemocyte-specific expression). Other fly lines used were generated through mating of the existing lines. I(2)mbn cells and S2 cells were maintained at 25 °C with Schneider's *Drosophila* medium (Invitrogen) containing 10% (v/v) heat-inactivated fetal bovine serum. I(2)mbn cells were used as phagocytes after they were incubated in the presence of 20-hydroxyecdysone (Sigma-Aldrich) (1 μM) for 2–5 days, essentially as described previously (Manaka *et al*, 2004). S2 cells were induced to undergo apoptosis by incubation with cycloheximide (1.5 μg/ml) for 24 h, as described previously (Manaka *et al*, 2004). To isolate larval hemocytes, hemolymph collected from wandering larvae was incubated on glass slides according to a published method (Pearson *et al*, 2003), and cells attaching to the slides were collected and used as hemocytes.

#### ***Affinity chromatography and mass spectrometry***

The region spanning amino acid residues 143–798 (with the amino terminus numbered 1) of Drpr-RB (based on the nomenclature in FlyBase), which probably corresponds to Drpr isoform I (Freeman *et al*, 2003), was expressed as a fusion protein with GST in Sf21 insect cells using the *Drosophila* EST clone GH03529 (provided by Berkeley *Drosophila* Genome Project and National Institute of Genetics) and a baculovirus-based DNA vector (Invitrogen), and the purified recombinant protein (Drpr-GST) was immobilized onto glutathione-Sepharose (Amersham Biosciences) using the cross-linking reagent DSP (Pierce). Apoptotic S2 cells were lysed with PIPES buffer (pH 6.5) containing 0.1 M NaCl, 20 mM KCl, 20 mM MgSO<sub>4</sub>, 10 mM CaCl<sub>2</sub> and 1% (w/v) CHAPS, and the lysates were applied onto the affinity matrix. The proteins retained on the matrix were eluted with 0.1 M Tris-glycine buffer (pH 2.7) containing 2 M NaCl, 1% CHAPS, 5 mM EDTA and 5 mM EGTA, and analyzed either by sodium dodecyl sulfate-polyacrylamide gel electrophoresis followed by staining with silver or Western blotting with anti-Prtp antibody. To identify a Drpr-binding protein, the protein band was excised and in-gel-digested with

*Achromobacter* protease I, and the resulting peptides were analyzed by LC-MS/MS using DiNa nano-flow liquid chromatograph (KYA Technologies, Tokyo) and Esquire HCT ion-trap mass spectrometer (Bruker Daltonics) with a nano-electrospray ionization probe.

### ***Assays for phagocytosis***

*In situ* analysis of phagocytosis was carried out with whole embryos by immunohistochemistry, TUNEL, ISNT, or a combination thereof, as described in the text. Ten intact embryos or dispersed cells obtained from about 200 embryos were analyzed in each experiment. An analysis of phagocytosis with dispersed embryonic cells was done as described previously (Manaka *et al*, 2004) except that a fluorochrome-based detection of signals was substituted by an enzyme-linked immunoassay, which modification made this assay highly reproducible, that is, results obtained from repeated experiments do not deviate over 10%. Phagocytosis reactions *in vitro* with I(2)mbn cells as phagocytes were carried out as described previously (Manaka *et al*, 2004). To prepare latex beads containing Prtp, fluorescein isothiocyanate-labeled latex beads ( $\Phi=1.7 \mu\text{m}$ ; Polysciences) were incubated with GST-fused Prtp, which had been expressed in and purified from *E. coli*, in the presence of the cross-linking reagent EDAC (Polysciences). For the surface expression of Prtp in S2 cells, a DNA coding for the amino acid residues 1–412 (with the amino terminus numbered 1) of Prtp that lacks the ER retention motif was linked with a DNA corresponding to the amino acid residues 606–626 of Dally (Takeo *et al*, 2005) by overlapping polymerase chain reaction using Dally cDNA (a gift from H Nakato) (see Supplementary Figure S10A). The resultant DNA was inserted into pUAST and introduced into S2 cells by the calcium/phosphate method together with pAct5C-GAL4 and pUAST-GFP (a gift from M Miura). Those S2 cells were mixed with 20-hydroxyecdysone-treated I(2)mbn cells (at 3 : 1), and the mixture was incubated at 25 °C for 1 h. The samples were washed and examined by microscopy after staining with hematoxylin, and I(2)mbn cells containing extra S2 cell nuclei were counted as those cells that had accomplished phagocytosis. To examine the basal phagocytic activity of

hemocytes, phagocytosis reactions were carried out using hemocytes isolated from wandering larvae as phagocytes and fluorescein isothiocyanate-labeled latex beads as targets.

### ***Other materials and methods***

Anti-Prtp antibody was raised by immunizing rats with GST-fused Prtp that had been expressed in *E. coli* and purified to homogeneity. The generation of anti-Drpr (Manaka *et al*, 2004), anti-Croquemort (Manaka *et al*, 2004), and anti-Ced-6 (Awasaki *et al*, 2006) antibodies was reported previously. Anti-Fasciclin II monoclonal antibody was provided by A Nose. Anti-Repo mouse monoclonal antibody 8D12 and anti- $\beta$ -galactosidase monoclonal antibody (used for fly genotyping in the experiments shown as Figure 3) were obtained from Developmental Studies Hybridoma Bank. Anti-GFP monoclonal antibody and anti-GFP polyclonal antibody were purchased from Roche and Molecular Probes, respectively. Anti- $\alpha$ -tubulin and anti-human activated caspase-3 antibodies were purchased from Sigma-Aldrich and Cell Signaling, respectively. z-VAD-fmk was obtained from R&D Systems. Varying portions of Prtp were expressed in *E. coli* as proteins fused with maltose-binding protein (MBP) and affinity purified to homogeneity using amylose-Sepharose (New England BioLabs). These proteins were incubated with Drpr-GST, precipitated with amylose-Sepharose, and analyzed for the association of Drpr-GST by Western blotting with anti-GST (Upstate) or anti-MBP (New England BioLabs) antibody. MBP-fused  $\beta$ -galactosidase was similarly prepared and used as a negative control. To examine the phosphorylation of Drpr, l(2)mbn cells ( $1 \times 10^7$ ) were maintained in culture containers ( $\Phi=6$  cm) that had been coated with MBP-fused Prtp (full length, 0.3 mg) or  $\beta$ -galactosidase at 25 °C for 5.5 h, washed with phosphate-buffered saline, and lysed with buffer consisting of 40 mM Tris-HCl (pH 7.5), 2% CHAPS, 0.15 M NaCl and 1 mM EDTA. The lysates were analyzed by immunoprecipitation with anti-Drpr antibody followed by Western blotting with anti-phosphotyrosine (clone RC20; BD Biosciences) or anti-Drpr antibody. Western blotting, RNA interference, cytochemistry with fluorochrome-labeled annexin V, and ISNT were carried out

as described previously (Manaka *et al*, 2004). TUNEL was done according to the manufacturer's instructions (Chemicon). Immunohistochemistry with cultured cells and embryos was done as described previously (Manaka *et al*, 2004; Kuraishi *et al*, 2007). To induce apoptosis in wing discs, late third-instar larvae of *UAS-rpr UAS-hid / + ; en-GAL4 / tub-GAL80<sup>ts</sup>* that had been maintained at 20 °C were kept at 29 °C for 12 h. The discs isolated from those larvae were immunohistochemically analyzed for the presence of Prtp and  $\alpha$ -tubulin with and without membrane permeabilization according to the method of Strigini and Cohen (2000). An analysis of axon pruning was done as described previously (Awasaki *et al*, 2006). Reverse transcription-mediated polymerase chain reaction was conducted according to a standard procedure with primers containing sequences of mRNA for Prtp and Drpr.

### ***Genotypes of the fly lines analyzed***

In Figures 2B, C, D, and F:

*w<sup>1118</sup> prtp<sup>G19</sup> / w<sup>1118</sup> prtp<sup>G19</sup> ; srpHemo-GAL4 UAS-srcEGFP / srpHemo-GAL4 UAS-srcEGFP (G19)*, *w<sup>1118</sup> prtp<sup>Δ1</sup> / w<sup>1118</sup> prtp<sup>Δ1</sup> ; srpHemo-GAL4 UAS-srcEGFP / srpHemo-GAL4 UAS-srcEGFP (Δ1)*, and *w<sup>1118</sup> prtp<sup>Δ2</sup> / w<sup>1118</sup> prtp<sup>Δ2</sup> ; srpHemo-GAL4 UAS-srcEGFP / srpHemo-GAL4 UAS-srcEGFP (Δ2)*.

In Figure 2E:

*w<sup>1118</sup> prtp<sup>G19</sup> / w<sup>1118</sup> prtp<sup>G19</sup> (+ / +)*, *w<sup>1118</sup> prtp<sup>Δ1</sup> / w<sup>1118</sup> prtp<sup>Δ1</sup> (prtp<sup>Δ1</sup>)*, *prtp<sup>Δ1</sup> / prtp<sup>Δ1</sup> ; da-GAL4 / + (prtp<sup>Δ1</sup> ; da-GAL4 / +)*, *prtp<sup>Δ1</sup> / prtp<sup>Δ1</sup> ; srpHemo-GAL4 UAS-srcEGFP / + (prtp<sup>Δ1</sup> ; srp-GAL4 / +)*, *prtp<sup>Δ1</sup> / prtp<sup>Δ1</sup> ; da-Gal4 / UAS-prtp (prtp<sup>Δ1</sup> ; da-GAL4 / UAS-prtp)*, and *prtp<sup>Δ1</sup> / prtp<sup>Δ1</sup> ; srpHemo-GAL4 UAS-srcEGFP / + ; UAS-prtp / + (prtp<sup>Δ1</sup> ; srp-GAL4 / + ; UAS-prtp / +)*.

In Figure 2G and I:

*w<sup>1118</sup> prtp<sup>G19</sup> / w<sup>1118</sup> prtp<sup>G19</sup> (G19)*, *w<sup>1118</sup> prtp<sup>Δ1</sup> / w<sup>1118</sup> prtp<sup>Δ1</sup> (Δ1)*, and *w<sup>1118</sup> prtp<sup>Δ2</sup> / w<sup>1118</sup> prtp<sup>Δ2</sup> (Δ2)*.

In Figure 2H:

$w^{1118} prtp^{G19} / w^{1118} prtp^{G19}$  ;  $Rep1^P / Rep1^P (G19)$ ,  $w^{1118} prtp^{\Delta1} / w^{1118} prtp^{\Delta1}$  ;  $Rep1^P / Rep1^P (\Delta1)$ ,  
and  $w^{1118} prtp^{\Delta2} / w^{1118} prtp^{\Delta2}$  ;  $Rep1^P / Rep1^P (\Delta2)$ .

In Figure 3A:

$w^{1118} prtp^{G19} / w^{1118} prtp^{G19} (+ / +)$ ,  $w^{1118} prtp^{\Delta1} / w^{1118} prtp^{\Delta1} (prtp^{\Delta1})$ ,  $w^{1118} prtp^{\Delta1} / w^{1118} prtp^{\Delta1}$  ;  
 $drpr^{\Delta5} / drpr^{\Delta5} (prtp^{\Delta1} ; drpr^{\Delta5})$ , and  $w^{1118} prtp^{\Delta1} / w^{1118} prtp^{\Delta1}$  ;  $ced-6^{J26} / ced-6^{J26} (prtp^{\Delta1}$  ;  
 $ced-6^{J26})$ .

In Figure 3B:

$w^{1118} / w^{1118} (+ / +)$ ,  $w^{1118} prtp^{\Delta1} / w^{1118} (prtp^{\Delta1} / +)$ ,  $w^{1118} / w^{1118}$  ;  $drpr^{\Delta5} / + (drpr^{\Delta5} / +)$ ,  $w^{1118} /$   
 $w^{1118}$  ;  $ced-6^{J26} / + (ced-6^{J26} / +)$ ,  $w^{1118} prtp^{\Delta1} / w^{1118}$  ;  $drpr^{\Delta5} / + (prtp^{\Delta1} / + ; drpr^{\Delta5} / +)$ ,  $w^{1118}$   
 $prtp^{\Delta1} / w^{1118}$  ;  $ced-6^{J26} / + (prtp^{\Delta1} / + ; ced-6^{J26} / +)$ , and  $w^{1118} prtp^{\Delta1} / Y (prtp^{\Delta1} hemi)$  for Western  
blotting, and  $w^{1118} / w^{1118}$  ;  $srpHemo-GAL4 UAS-srcEGFP / + (+ / +)$ ,  $w^{1118} prtp^{\Delta1} / w^{1118}$  ;  
 $srpHemo-GAL4 UAS-srcEGFP / + (prtp^{\Delta1} / +)$ ,  $w^{1118} / w^{1118}$  ;  $srpHemo-GAL4 UAS-srcEGFP / +$  ;  
 $drpr^{\Delta5} / + (drpr^{\Delta5} / +)$ ,  $w^{1118} / w^{1118}$  ;  $ced-6^{J26} / srpHemo-GAL4 UAS-srcEGFP (ced-6^{J26} / +)$ ,  $w^{1118}$   
 $prtp^{\Delta1} / w^{1118}$  ;  $srpHemo-GAL4 UAS-srcEGFP / + ; drpr^{\Delta5} / + (prtp^{\Delta1} / + ; drpr^{\Delta5} / +)$ ,  $w^{1118} prtp^{\Delta1} /$   
 $w^{1118}$  ;  $ced-6^{J26} / srpHemo-GAL4 UAS-srcEGFP (prtp^{\Delta1} / + ; ced-6^{J26} / +)$ , and  $w^{1118} prtp^{\Delta1} / Y$  ;  
 $srpHemo-GAL4 UAS-srcEGFP / + (prtp^{\Delta1} hemi)$  for phagocytosis analysis.

In Figure 3C:

$prtp^{G19} / prtp^{G19}$  ;  $srpHemo-GAL4 UAS-srcEGFP / + (+ / +)$ ,  $srpHemo-GAL4 UAS-srcEGFP / +$  ;  
 $red^1 e^1 mbc^{C1} / + (mbc^{C1} / +)$ ,  $srpHemo-GAL4 UAS-srcEGFP / +$  ;  $Rac^{J11} Rac2^{\Delta} FRT2A / + (Rac^{J11}$   
 $Rac2^{\Delta} / +)$ ,  $w^{1118} prtp^{\Delta1} / w^{1118} prtp^{G19}$  ;  $srpHemo-GAL4 UAS-srcEGFP / + (prtp^{\Delta1} / +)$ ,  $prtp^{\Delta1} / +$  ;  
 $srpHemo-GAL4 UAS-srcEGFP / +$  ;  $red^1 e^1 mbc^{C1} / + (prtp^{\Delta1} / + ; mbc^{C1} / +)$ ,  $prtp^{\Delta1} / +$  ;  
 $srpHemo-GAL4 UAS-srcEGFP / +$  ;  $Rac^{J11} Rac2^{\Delta} FRT2A / + (prtp^{\Delta1} / + ; Rac^{J11} Rac2^{\Delta} / +)$ , and  
 $w^{1118} prtp^{\Delta1} / Y$  ;  $srpHemo-GAL4 UAS-srcEGFP / + (prtp^{\Delta1} hemi)$ .

In Figure 3D:

*y w (+ / +), elmo<sup>KO</sup> FRT40, 42 / elmo<sup>KO</sup> FRT40, 42 (elmo<sup>KO</sup>).*

### ***Data processing and statistical analysis***

Data in a numerical analysis are expressed as the mean  $\pm$  s.d. of the results obtained from at least three independent experiments, unless otherwise mentioned in the text. Other data are representative of at least two independent experiments that yielded similar results. For determining the level of phagocytosis, two investigators independently conducted the same experiments or the data obtained by one investigator were re-examined in blind by another, and only the replicated results were presented in this paper. Statistical analyses were performed using the Student's *t*-test and *P* values of  $< 0.05$  were considered significant.

### ***Supplementary information***

Supplementary data are available at *The EMBO Journal* Online.

## Acknowledgements

We thank B Dickson, M Freeman, S Hayashi, M Meister, S Nagata, and Bloomington Stock Center for the fly stocks; M Miura and H Nakato for the DNA; Berkeley Drosophila Genome Project and National Institute of Genetics for the EST clones; and A Nose and Developmental Studies Hybridoma Bank for the antibodies. We are grateful to M-O Fauvarque, S Hayashi, K Ito, K Koizumi, E Kuranaga, S Kurata, M Miura, Y Nakai, R Tajiri, L Tsuda, R Ueda, and Y Yoshioka for advice and suggestions, and M Freeman, S Hayashi, K Ito, H Kanuka, and Y-C Wu for discussion. We thank R Tatsumi for technical support. We also acknowledge the use of FlyBase. This study was supported by Grants-in-Aid for Scientific Research from the Japan Society for the Promotion of Science (grant number 19370051 to YN), and in part by Grants-in-Aid for Scientific Research from the Japan Society for the Promotion of Science (grant number 18570123 to AS) and from the Ministry of Education, Culture, Sports, Science and Technology-Japan (grant number 18057009 to AS). TK was a recipient of the predoctoral fellowship from the Japan Society for the Promotion of Science. All the authors performed the experiments and analyzed the data. TK and YN designed the study. YN supervised the study. TK, YN, and TA prepared the manuscript. The authors declare no competing financial interests.

## References

- Abrams JM, White K, Fessler LI, Steller H (1993) Programmed cell death during *Drosophila* embryogenesis. *Development* **117**: 29–43
- Awasaki T, Tatsumi R, Takahashi K, Arai K, Nakanishi Y, Ueda R, Ito K (2006) Essential role of the apoptotic cell engulfment genes *draper* and *ced-6* in programmed axon pruning during *Drosophila* metamorphosis. *Neuron* **50**: 855–867
- Bianco A, Poukkula M, Cliffe A, Mathieu J, Luque CM, Fulga TA, Rørth P (2007) Two distinct modes of guidance signalling during collective migration of border cells. *Nature* **448**: 362–365
- Brand AH, Perrimon N (1993) Targeted gene expression as a means of altering cell fates and generating dominant phenotypes. *Development* **118**: 401–415
- Brückner K, Kockel L, Duchek P, Luque CM, Rørth P, Perrimon N (2004) The PDGF/VEGF receptor controls blood cell survival in *Drosophila*. *Dev Cell* **7**: 73–84
- Callebaut I, Mignotte V, Souchet M, Mornon J-P (2003) EMI domains are widespread and reveal the probable orthologs of the *Caenorhabditis elegans* CED-1 protein. *Biochem Biophys Res Commun* **300**: 619–623
- Cleveland DW (1996) Neuronal growth and death: order and disorder in the axoplasm. *Cell* **84**: 663–666
- Cohen JJ (1991) Programmed cell death in the immune system. *Adv Immunol* **50**: 55–85
- Cuttell L, Vaughan A, Silva E, Escaron CJ, Lavine M, Van Goethem E, Eid J-P, Quirin M, Franc NC (2008) Undertaker, a *Drosophila* Junctophilin, links Draper-mediated phagocytosis and calcium homeostasis. *Cell* **135**: 524–534
- Fadok VA, Bratton DL, Frasch SC, Warner ML, Henson PM (1998) The role of phosphatidylserine in recognition of apoptotic cells by phagocytes. *Cell Death Differ* **5**: 551–562
- Franc NC, Dimarcq J-L, Lagueux M, Hoffmann J, Ezekowitz RAB (1996) Croquemort, a novel *Drosophila* hemocyte/macrophage receptor that recognizes apoptotic cells. *Immunity* **4**: 431–443

- Franc NC, Heitzler P, Ezekowitz RAB, White K (1999) Requirement for Croquemort in phagocytosis of apoptotic cells in *Drosophila*. *Science* **284**: 1991–1994
- Franz S, Herrmann K, Führrohr B, Sheriff A, Frey B, Gaipf US, Voll RE, Kalden JR, Jäck H-M, Herrmann M (2007) After shrinkage apoptotic cells expose internal membrane-derived epitopes on their plasma membranes. *Cell Death Differ* **14**: 733–742
- Freeman MR, Delrow J, Kim J, Johnson E, Doe CQ (2003) Unwrapping glial biology: Gcm target genes regulating glial development, diversification, and function. *Neuron* **38**: 567–580
- Giebel B, Stüttem I, Hinz U, Campos-Ortega JA (1997) Lethal of Scute requires overexpression of Daughterless to elicit ectopic neuronal development during embryogenesis in *Drosophila*. *Mech Develop* **63**: 75–87
- Hakeda-Suzuki S, Ng J, Tzu J, Dietzl G, Sun Y, Harms M, Nardine T, Luo L, Dickson BJ (2002) Rac function and regulation during *Drosophila* development. *Nature* **416**: 438–442
- Hamon Y, Trompier D, Ma Z, Venegas V, Pophillat M, Mignotte V, Zhou Z, Chimini G (2006) Cooperation between engulfment receptors: the case of ABCA1 and MEGF10. *PLoS ONE* **1**: e120
- Hashimoto Y, Tabuchi Y, Sakurai K, Kutsuna M, Kurokawa K, Awasaki T, Sekimizu K, Nakanishi Y, Shiratsuchi A (2009) Identification of lipoteichoic acid as a ligand for Draper in the phagocytosis of *Staphylococcus aureus* by *Drosophila* hemocytes. *J Immunol* in press
- Jacobson MD, Weil M, Raff MC (1997) Programmed cell death in animal development. *Cell* **88**: 347–354
- Kinchen JM, Cabello J, Klingele D, Wong K, Feichtinger R, Schnabel H, Schnabel R, Hengartner MO (2005) Two pathways converge at CED-10 to mediate actin rearrangement and corpse removal in *C. elegans*. *Nature* **434**: 93–99
- Kinchen JM, Hengartner MO (2005) Tales of cannibalism, suicide, and murder: programmed cell death in *C. elegans*. *Curr Top Dev Biol* **65**: 1–45
- Kinchen JM, Ravichandran KS (2007) Journey to the grave: signaling events regulating removal of

- apoptotic cells. *J Cell Sci* **120**: 2143–2149
- Knoblach B, Keller BO, Groenendyk J, Aldred S, Zheng J, Lemire BD, Li L, Michalak M (2003) ERp19 and ERp46, new members of the thioredoxin family of endoplasmic reticulum proteins. *Mol Cell Proteomics* **2**: 1104–1119
- Kuraishi T, Manaka J, Kono M, Ishii H, Yamamoto N, Koizumi K, Shiratsuchi A, Lee BL, Higashida H, Nakanishi Y (2007) Identification of calreticulin as a marker for phagocytosis of apoptotic cells in *Drosophila*. *Exp Cell Res* **313**: 500–510
- Kurant E, Axelrod S, Leaman D, Gaul U (2008) Six-microns-under acts upstream of Draper in the glial phagocytosis of apoptotic neurons. *Cell* **133**: 498–509
- LaJeunesse DR, Buckner SM, Lake J, Na C, Pirt A, Fromson K (2004) Three new *Drosophila* markers of intracellular membranes. *Biotechniques* **36**: 784–790
- Lauber K, Blumenthal SG, Waibel M, Wesselborg S (2004) Clearance of apoptotic cells: getting rid of the corpses. *Mol Cell* **14**: 277–287
- Lettre G, Hengartner MO (2006) Developmental apoptosis in *C. elegans*: a complex CEDnario. *Nat Rev Mol Cell Biol* **7**: 97–108
- Levine T, Rabouille C (2005) Endoplasmic reticulum: one continuous network compartmentalized by extrinsic cues. *Curr Opin Cell Biol* **17**: 362–368
- Liao DJ (2005) The scavenger cell hypothesis of apoptosis: Apoptosis redefined as a process by which a cell in living tissue is destroyed by phagocytosis. *Med Hypotheses* **65**: 23–28
- MacDonald JM, Beach MG, Porpiglia E, Sheehan AE, Watts RJ, Freeman MR (2006) The *Drosophila* cell corpse engulfment receptor Draper mediates glial clearance of severed axons. *Neuron* **50**: 869–881
- Manaka J, Kuraishi T, Shiratsuchi A, Nakai Y, Higashida H, Henson P, Nakanishi Y (2004) Draper-mediated and phosphatidylserine-independent phagocytosis of apoptotic cells by *Drosophila* hemocytes/macrophages. *J Biol Chem* **279**: 48466–48476
- Mangahas PM, Zhou Z (2005) Clearance of apoptotic cells in *Caenorhabditis elegans*. *Sem Cell*

*Dev Biol* **16**: 295–306

McGuire SE, Le PT, Osborn AJ, Matsumoto K, Davis RL (2003) Spatiotemporal rescue of memory dysfunction in *Drosophila*. *Science* **302**: 1765–1768

Mukae N, Yokoyama H, Yokokura T, Sakoyama Y, Nagata S (2002) Activation of the innate immunity in *Drosophila* by endogenous chromosomal DNA that escaped apoptotic degradation. *Genes Dev* **16**: 2662–2671

Milán M, Campuzano S, García-Bellido A (1997) Developmental parameters of cell death in the wing disc of *Drosophila*. *Proc Natl Acad Sci USA* **94**: 5691–5696

Nakanishi Y, Henson PM, Shiratsuchi A (2009) Pattern recognition in phagocytic clearance of altered self. In *Target Pattern Recognition in Innate Immunity*, Kishore U (ed) pp 129–138. Austin: Landes Bioscience

Ng J, Nardine T, Harms M, Tzu J, Goldstein A, Sun Y, Dietzl G, Dickson BJ, Luo L (2002) Rac GTPases control axon growth, guidance and branching. *Nature* **416**: 442–447

Nissom PM, Lo SL, Lo JCY, Ong PF, Lim JWE, Ou K, Liang RC, Seow TK, Chung MCM (2006) Hcc-2, a novel mammalian ER thioredoxin that is differentially expressed in hepatocellular carcinoma. *FEBS Lett* **580**: 2216–2226

Nolan KM, Barrett K, Lu Y, Hu K-Q, Vincent S, Settleman J (1998) Myoblast city, the *Drosophila* homolog of DOCK180/CED-5, is required in a Rac signaling pathway utilized for multiple developmental processes. *Genes Dev* **12**: 3337–3342

Panaretakis T, Kepp O, Brockmeier U, Tesniere A, Bjorklund A-C, Chapman DC, Durchschlag M, Joza N, Pierron G, van Endert P, Yuan J, Zitvogel L, Madeo F, Williams DB, Kroemer G (2009) Mechanisms of pre-apoptotic calreticulin exposure in immunogenic cell death. *EMBO J* **28**: 578–590

Pearson AM, Baksa K, Rämets M, Protas M, McKee M, Brown D, Ezekowitz RAB (2003) Identification of cytoskeletal regulatory proteins required for efficient phagocytosis in *Drosophila*. *Microbes Infect* **5**: 815–824

- Prokopenko SN, He Y, Lu Y, Bellen HJ (2000) Mutations affecting the development of the peripheral nervous system in *Drosophila*: a molecular screen for novel proteins. *Genetics* **156**: 1691–1715
- Ravichandran KS, Lorenz U (2007) Engulfment of apoptotic cells: signals for a good meal. *Nat Rev Immunol* **7**: 964–974
- Reddien PW, Horvitz HR (2004) The engulfment process of programmed cell death in *Caenorhabditis elegans*. *Annu Rev Cell Dev Biol* **20**: 193–221
- Robertson HM, Preston CR, Phillis RW, Johnson-Schlitz DM, Benz WK, Engels WR (1988) A stable genomic source of *P* element transposase in *Drosophila melanogaster*. *Genetics* **118**: 461–470
- Rushton E, Drysdale R, Abmayr SM, Michelson AM, Bate M (1995) Mutations in a novel gene, *myoblast city*, provide evidence in support of the founder cell hypothesis for *Drosophila* muscle development. *Development* **121**: 1979–1988
- Savill J, Fadok V (2000) Corpse clearance defines the meaning of cell death. *Nature* **407**: 784–788
- Schlegel RA, Williamson P (2001) Phosphatidylserine, a death knell. *Cell Death Differ* **8**: 551–563
- Silva E, Au-Yeung HW, Goethem EV, Burden J, Franc NC (2007) Requirement for a *Drosophila* E3-ubiquitin ligase in phagocytosis of apoptotic cells. *Immunity* **27**: 585–596
- Sonnenfeld MJ, Jacobs JR (1995) Macrophages and glia participate in the removal of apoptotic neurons from the *Drosophila* embryonic nervous system. *J Comp Neurol* **359**: 644–652
- Spradling AC (1986) P element-mediated transformation. In *Drosophila: A Practical Approach Second Edition*, Roberts DB (ed) pp 175–197. Leeds: Oxford University Press
- Strigini M, Cohen SM (2000) Wingless gradient formation in the *Drosophila* wing. *Curr Biol* **10**: 293–300
- Tabata T, Schwartz C, Gustavson E, Ali Z, Kornberg TB (1995) Creating a *Drosophila* wing de novo, the role of *engrailed*, and the compartment border hypothesis. *Development* **121**: 3359–3369

- Vaux DL, Korsmeyer SJ (1999) Cell death in development. *Cell* **96**: 245–254
- Venegas V, Zhou Z (2007) Two alternative mechanisms that regulate the presentation of apoptotic cell engulfment signal in *Caenorhabditis elegans*. *Mol Biol Cell* **18**: 3180–3192
- Wyllie AH, Kerr JFR, Currie AR (1980) Cell death: the significance of apoptosis. *Int Rev Cytol* **68**: 251–306
- Yang MY, Armstrong JD, Vilinsky I, Strausfeld NJ, Kaiser K (1995) Subdivision of the *Drosophila* mushroom bodies by enhancer-trap expression patterns. *Neuron* **15**: 45–54
- Yu X, Odera S, Chuang C-H, Lu N, Zhou Z (2006) *C. elegans* dynamin mediates the signaling of phagocytic receptor CED-1 for the engulfment and degradation of apoptotic cells. *Dev Cell* **10**: 743–757
- Zhou L, Schnitzler A, Agapite J, Schwartz LM, Steller H, Nambu JR (1997) Cooperative functions of the *reaper* and *head involution defective* genes in the programmed cell death of *Drosophila* central nervous system midline cells. *Proc Natl Acad Sci USA* **94**: 5131–5136
- Zhou Z, Hartweg E, Horvitz HR (2001) CED-1 is a transmembrane receptor that mediates cell corpse engulfment in *C. elegans*. *Cell* **104**: 43–56
- Ziegenfuss JS, Biswas R, Avery MA, Hong K, Sheehan AE, Yeung Y-G, Stanley ER, Freeman MR (2008) Draper-dependent glial phagocytic activity is mediated by Src and Syk family kinase signalling. *Nature* **453**: 935–939

## Figure legends

**Figure 1** Isolation of Prtp as a Drpr-binding ER protein. (A) Sodium dodecyl sulfate-polyacrylamide gel electrophoresis (stained with silver) of bound materials in chromatography of whole-cell lysates of S2 cells, which were induced to undergo apoptosis by the treatment with cycloheximide, on Sepharose conjugated with the indicated proteins. The arrowhead denotes the protein band brought to mass spectrometry. Shown at the bottom are magnified views of the squared areas. (B) Predicted domain structure of Prtp (shaded, hatched, and closed boxes denote signal peptide, thioredoxin-like domain (TLD), and ER retention motif, respectively). The regions of Prtp tested for the binding to Drpr in (D) are indicated. (C) Western blotting of the samples in (A) with anti-Prtp antibody. (D) Cell-free analysis of the binding of Prtp to the extracellular region of Drpr. The indicated MBP-fused proteins were incubated with Drpr-GST, pulled down, and analyzed by Western blotting with anti-GST or anti-MBP antibody. (E) Expression of Prtp and Drpr analyzed by Western blotting with lysates of whole animals at the indicated developmental stages. (F) Immunochemical analysis of Prtp expression with embryos and dispersed embryonic cells at stage 16. Bars, 100  $\mu$ m. (G) Subcellular localization of Prtp in an embryonic cell expressing yellow fluorescent protein containing the ER retention signal KDEL (LaJeunesse *et al*, 2004). Bar, 2  $\mu$ m.

**Figure 2** Requirement of Prtp in apoptotic cell phagocytosis by hemocytes and glia. (A) Generation of *prtp* null mutants. The structure of the *Drosophila* genome near *prtp* (exons are indicated by boxes with protein-coding regions shaded) and the positions of deletions in mutant flies are schematically shown. After P-element excision with *CG1837*<sup>BG00450</sup>, two fly lines with deletions in the first exon of *prtp*, *prtp* <sup>$\Delta$ 1</sup> ( $\Delta$ 1) (with a deletion in the region between nucleotide positions -45 and +354 with the transcription start site numbered as +1) and *prtp* <sup>$\Delta$ 2</sup> ( $\Delta$ 2) (with a deletion in the region from -45 to +1170), and one line, *prtp*<sup>G19</sup> (G19), that lost the P-element with

no alteration in *prtp* were isolated. **(B)** Distribution (left) and number (right) (dispersed cells were analyzed) of GFP-positive hemocytes in embryos of the indicated fly lines. Data are from one of 2 independent experiments that yielded similar results. Bar, 20  $\mu\text{m}$ . **(C, D)** Level of phagocytosis by GFP-positive hemocytes determined with embryos (C) or dispersed embryonic cells (D) of the indicated fly lines. Signals of GFP and TUNEL are seen in blue and brown, respectively. The arrowhead points to a hemocyte containing a TUNEL-positive nucleus. The inset in (C) is a magnified view of the squared area. Bars, 10  $\mu\text{m}$  (C) and 2  $\mu\text{m}$  (D).  $*P < 0.01$  (vs. *G19*). **(E)** Level of phagocytosis by Croquemort-expressing hemocytes in embryos of the indicated fly lines.  $*P < 0.01$ . *ns*, difference not significant. **(F)** Level of phagocytosis of latex beads by larval hemocytes of the indicated fly lines. **(G)** Distribution (left) and number (right) (dispersed cells were analyzed) of Repo-positive glia in embryos of the indicated fly lines. Data are from one of 2 independent experiments that yielded similar results. Bar, 20  $\mu\text{m}$ . **(H, I)** Level of apoptotic cell phagocytosis by glia in the indicated fly lines. Embryos were analyzed for the number of ISNT-positive cells in the vicinity of the ventral nerve cord (depicted with a black line in the left panel of (G)) where glia are enriched (H), and dispersed embryonic cells were examined for the ratio of cells positive for both Repo (seen in blue) and TUNEL (seen in brown) against total Repo-positive cells (I). Bar, 2  $\mu\text{m}$ .  $*P < 0.01$  (vs. *G19*). Refer to Materials and methods for genotypes of the fly lines analyzed.

**Figure 3** Genetic interaction of *prtp* with *drpr*, *ced-6*, and *Rac1/Rac2*. **(A)** Level of phagocytosis by Croquemort-expressing hemocytes in embryos of the indicated fly lines. The data with control (+ / +) and *prtp<sup>Δ1</sup>* flies are duplications of those in Figure 2E. *ns* (difference not significant) vs. *prtp<sup>Δ1</sup>*. **(B)** Levels of proteins (top, Western blotting) and phagocytosis by GFP-positive hemocytes (bottom), determined with dispersed embryonic cells of the indicated fly lines. *prtp<sup>Δ1</sup> hemi* is a hemizygote lacking *prtp* expression.  $*P < 0.005$  (vs. *prtp<sup>Δ1</sup> / +*). **(C)** Level of phagocytosis by GFP-positive hemocytes in embryos of the indicated fly lines.  $*P < 0.05$

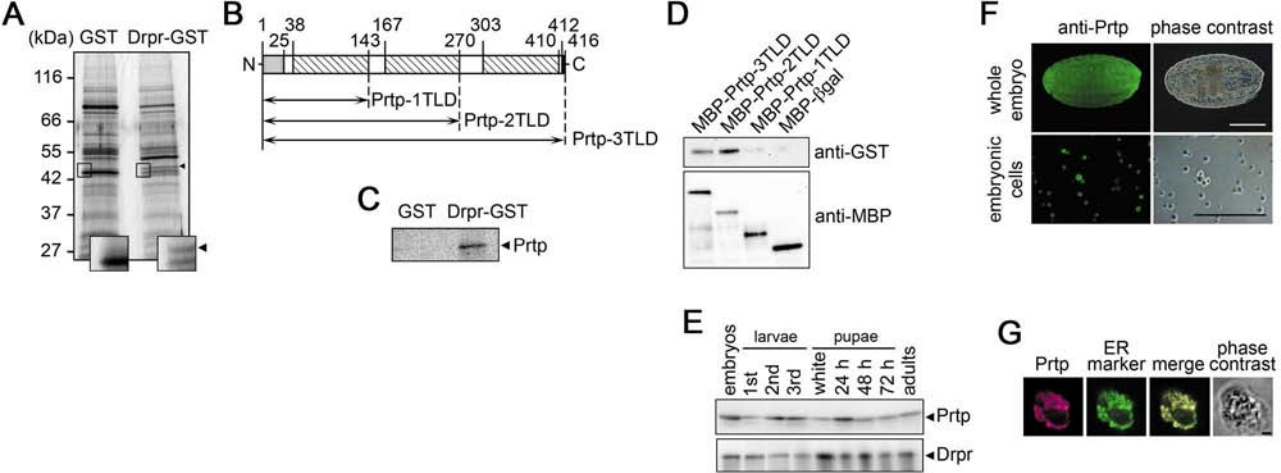
(vs. *prtp<sup>Δ1</sup> / +*). **(D)** Levels of phagocytosis, Croquemort-positive hemocytes, and TUNEL-positive apoptotic cells determined with dispersed embryonic cells of the indicated fly lines. Refer to Materials and methods for genotypes of the fly lines analyzed.

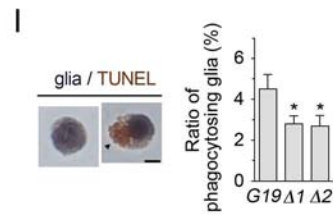
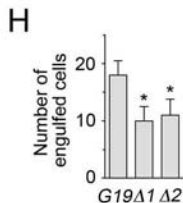
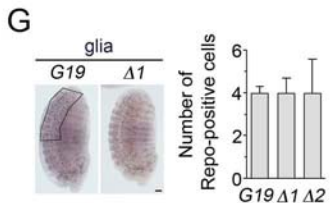
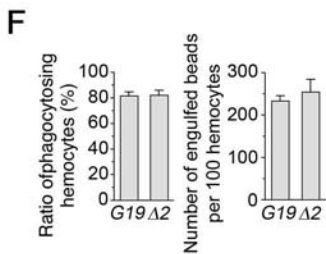
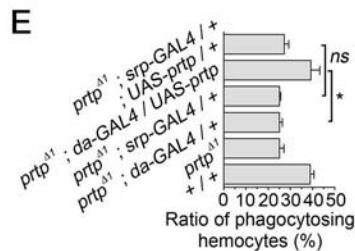
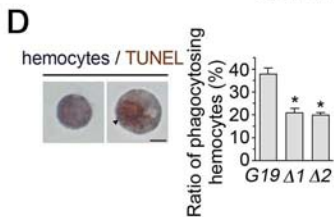
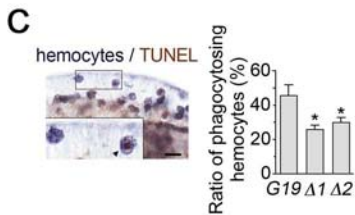
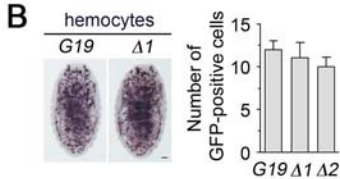
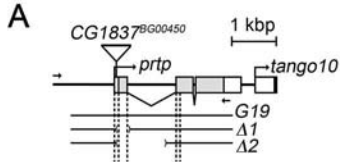
**Figure 4** Relocation of Prtp to the cell surface during apoptosis. **(A)** Surface expression of Prtp in S2 cells treated with cycloheximide (apoptotic) or left untreated (viable). Phase-contrast (bottom) and fluorescence (top) views of the same microscopic fields are shown. The inset is a magnified view of the squared area. Bar, 10  $\mu\text{m}$ . **(B)** Surface expression of Prtp in embryonic cells undergoing apoptosis. Apoptosis was induced in embryos of *UAS-rpr UAS-hid / + ; da-GAL4 / tub-GAL80<sup>Δs</sup>* flies by incubation at 29 °C for 11 h after egg laying. Cells obtained from those embryos were analyzed for the exposure of Prtp (using anti-Prtp antibody) and phosphatidylserine (PS) (using fluorochrome-labeled annexin V) under membrane-nonpermeabilizing conditions. Incubation with the probes was done in the absence and presence of EDTA, which chelates  $\text{Ca}^{2+}$  necessary for the binding of annexin V to phosphatidylserine. Phase-contrast and fluorescence views of the same microscopic fields are shown in each row. Bar, 5  $\mu\text{m}$ . **(C)** Surface expression of Prtp in apoptotic cells of wing discs. Wing discs, in which apoptosis was locally induced, were immunohistochemically analyzed for the expression of Prtp and tubulin with (total) and without (extracellular) membrane permeabilization. Apoptotic cells were detected by ISNT (Apoptosis). Fluorescence views of the same microscopic fields are shown in each row. The insets in the top row are magnified views of the corresponding squared area. Bar, 50  $\mu\text{m}$ .

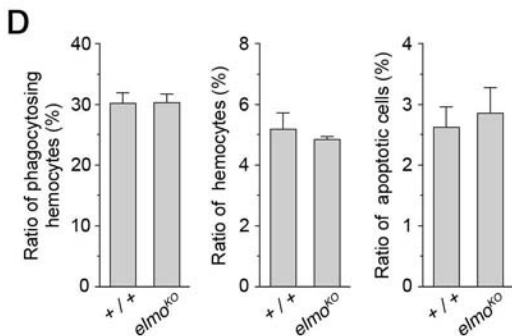
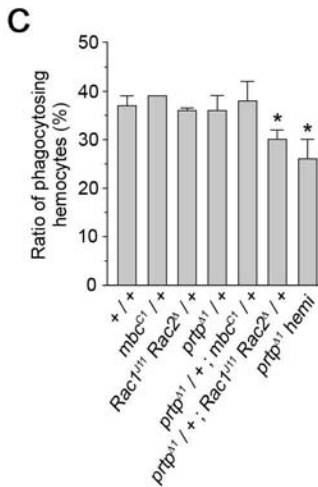
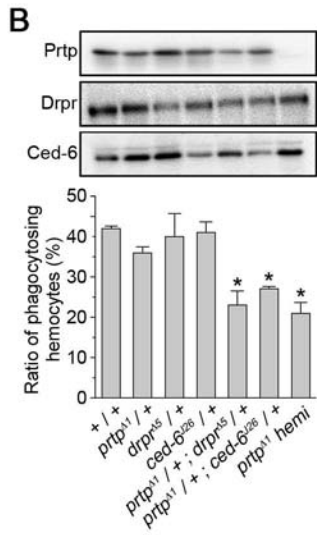
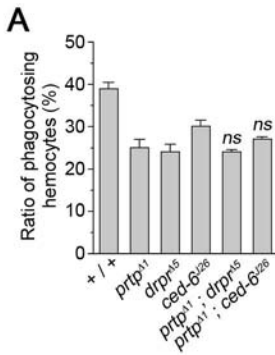
**Figure 5** Timing of Prtp externalization and other biochemical changes during apoptosis. **(A)** S2 cells induced to undergo apoptosis by the treatment with cycloheximide were examined for the occurrence of biochemical changes associated with apoptosis at the indicated time points. Phase-contrast and fluorescence views of the same microscopic fields in each analysis are shown.

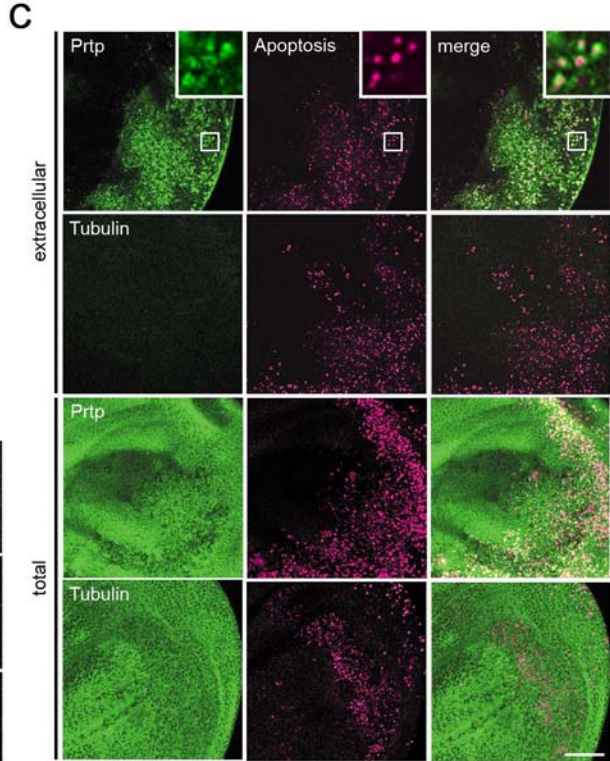
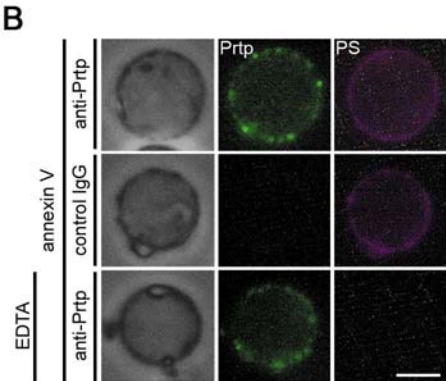
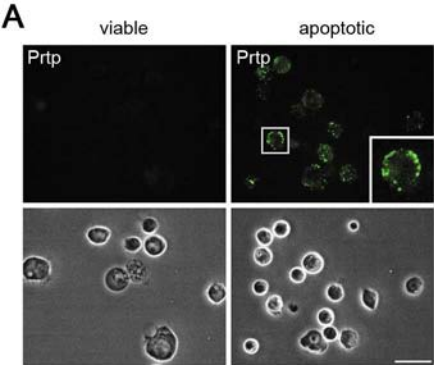
Bar, 10  $\mu\text{m}$ . The biochemical changes examined were: externalization of Prtp (analyzed by the binding of anti-Prtp antibody), externalization of phosphatidylserine (PS) (analyzed by the binding of annexin V), activation of pro-caspase-3 (casp-3) (immunochemically analyzed with anti-activated caspase-3 antibody), and fragmentation of DNA (analyzed by ISNT). **(B)** S2 cells were induced to undergo apoptosis by the treatment with cycloheximide in the presence and absence of the pan-caspase inhibitor z-VAD-fmk and examined for the occurrence of Prtp externalization. Bar, 10  $\mu\text{m}$ .

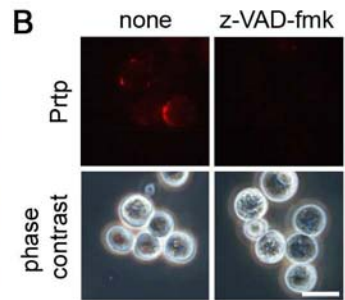
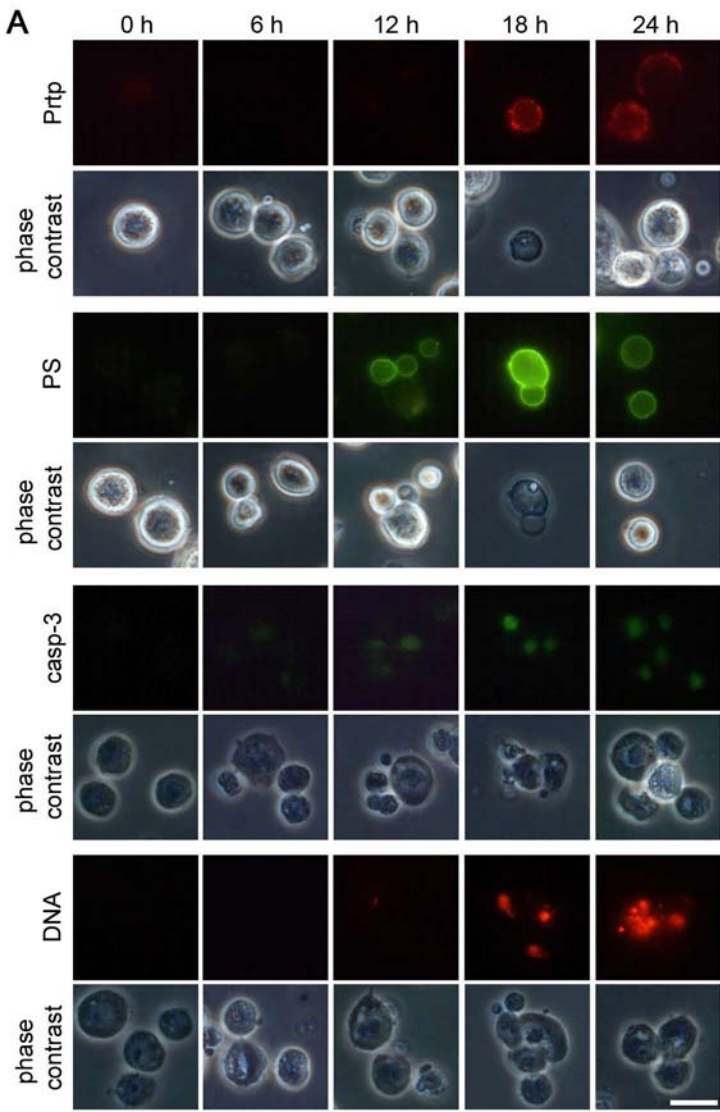
**Figure 6** Role of Prtp as a ligand for Drpr. **(A)** Phagocytosis of latex beads coated with Prtp. Latex beads coated with the indicated proteins were subjected to phagocytosis by l(2)mbn cells with and without RNA interference (dsRNA) of Drpr or Croquemort (Crq). Data are representative of 3 (none, Drpr) or 2 (Crq) independent experiments that yielded similar results. **(B)** Phagocytosis of S2 cells surface-expressing Prtp. S2 cells, which had been transfected with plasmid for the expression of glycosylphosphatidylinositol (GPI)-anchored Prtp and GFP, were examined for the presence of GFP and Prtp (left) and the phagocytosis by l(2)mbn cells (right). Phase contrast and fluorescent views of the same microscopic fields are shown in each row (left). Bar, 10  $\mu\text{m}$ . **(C)** Tyrosine phosphorylation of Drpr. l(2)mbn cells incubated with MBP-fused Prtp or  $\beta$ -galactosidase were subjected to an analysis of immunoprecipitation (IP) / Western blotting (Blot) using anti-Drpr and anti-phosphotyrosine (p-Tyr) antibodies.

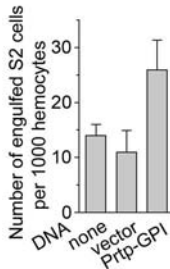
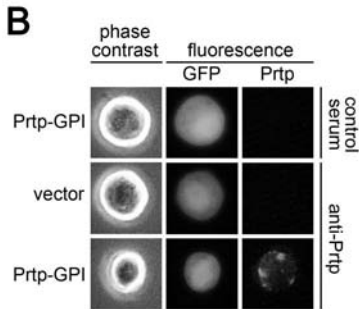
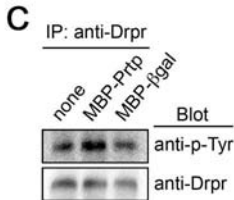
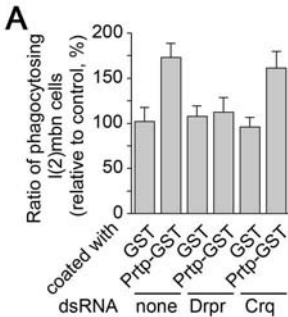


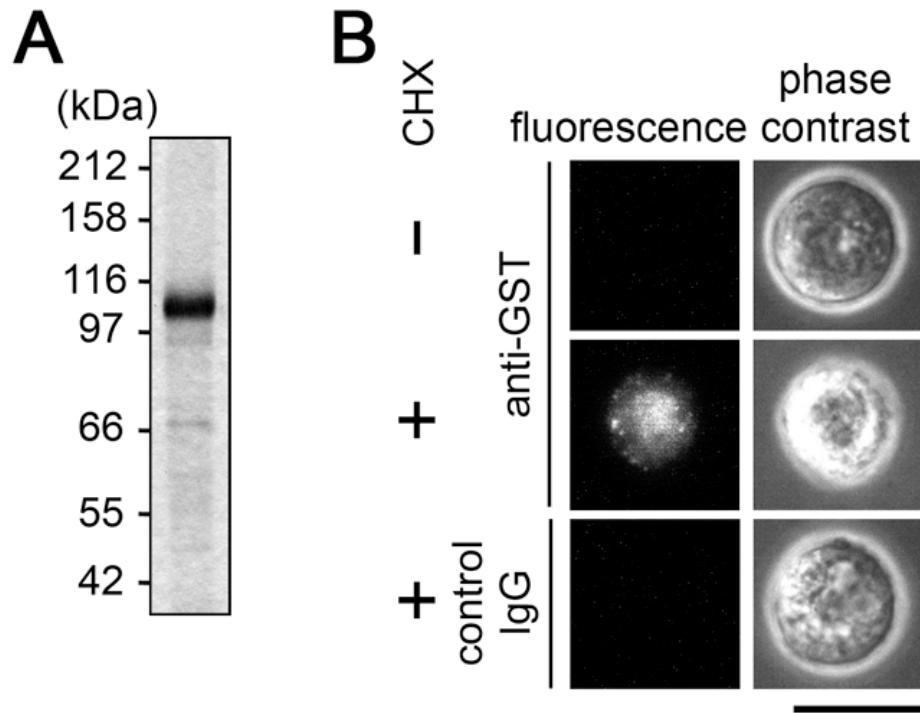




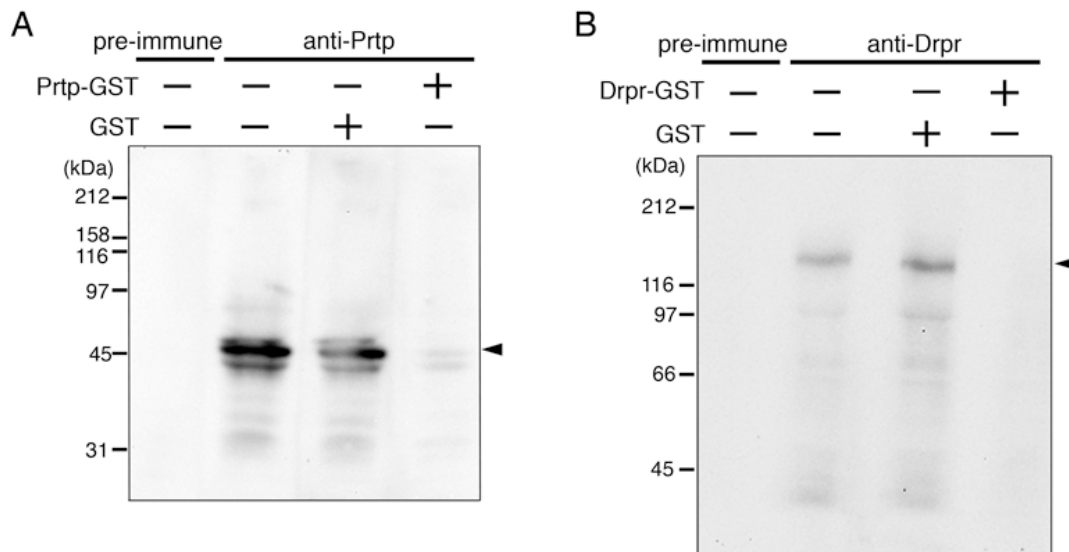




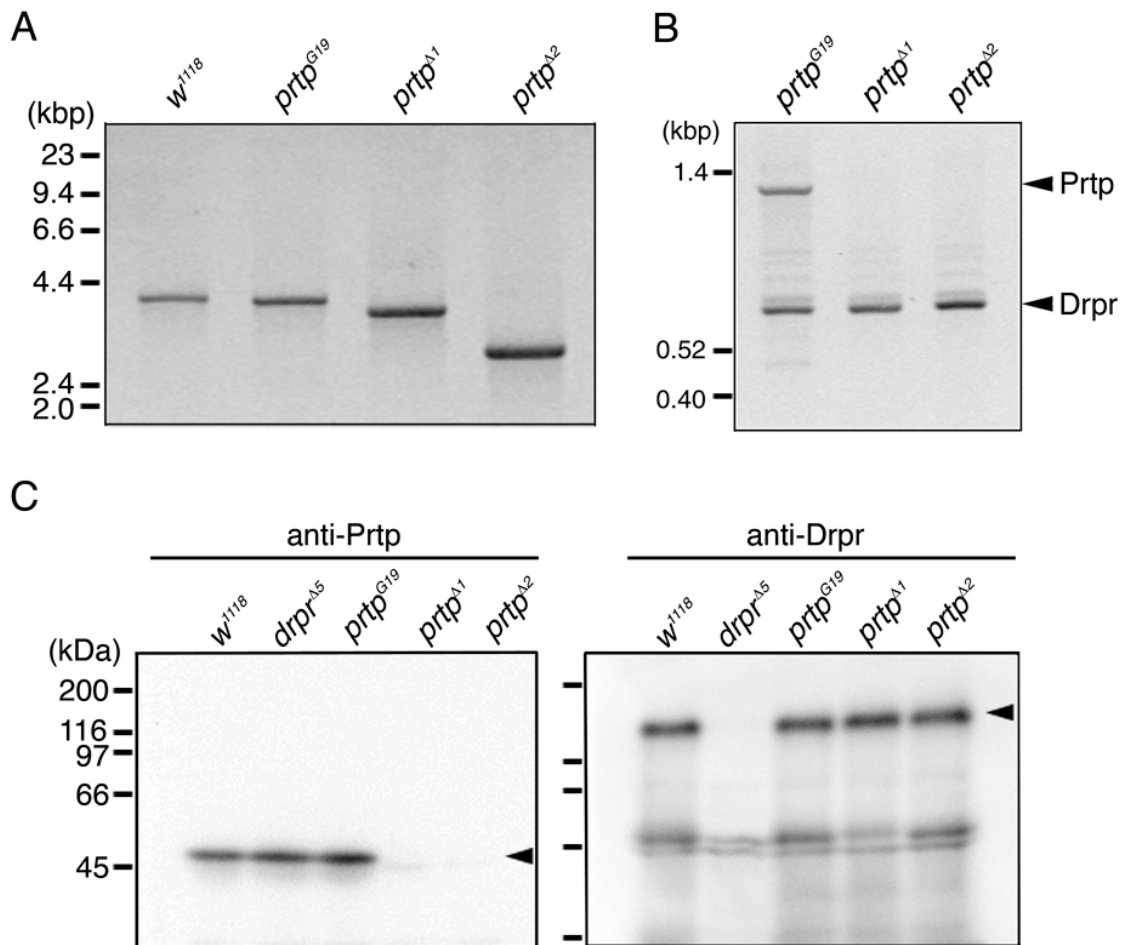




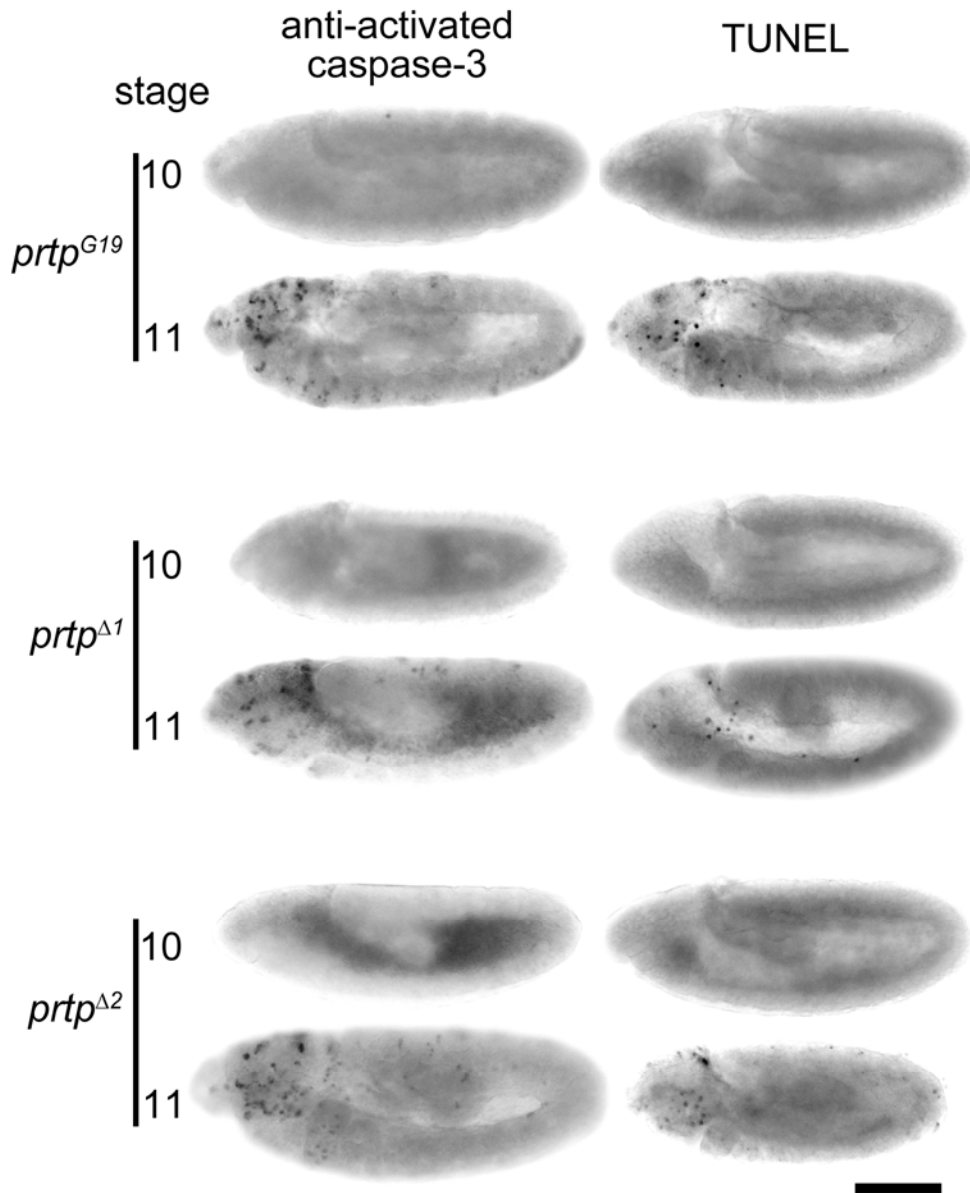
**Supplementary Figure S1** Binding of Drpr-GST to apoptotic cells. (A) Sodium dodecyl sulfate-polyacrylamide gel electrophoresis of an extracellular portion of Drpr fused to GST (Drpr-GST) (stained with Coomassie brilliant blue). (B) Immunofluorescence analysis of the binding of Drpr-GST to S2 cells. S2 cells, which had been treated with cycloheximide (CHX) for the induction of apoptosis or left untreated, were incubated with Drpr-GST, washed, and immunofluorescently analyzed with anti-GST antibody or control IgG. Fluorescence and phase contrast views of the same microscopic fields are shown in each row. Bar, 10  $\mu$ m.



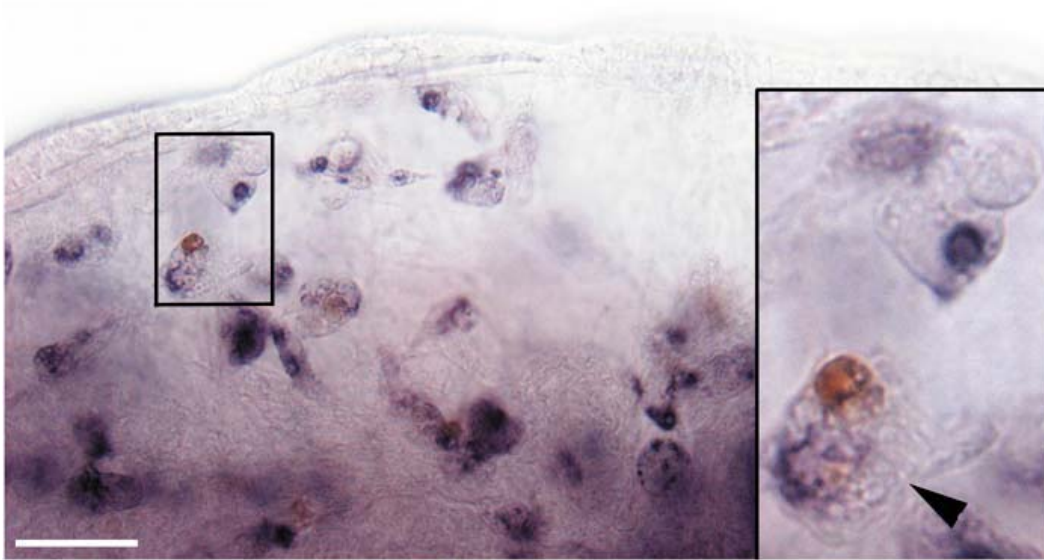
**Supplementary Figure S2** Antigen specificity of anti-Prtp and anti-Drpr antibodies in Western blotting. Whole-cell lysates of S2 cells (130  $\mu$ g protein) were analyzed by Western blotting with anti-Prtp, anti-Drpr, or the corresponding pre-immune serum of the rat. The antisera were pre-incubated with GST-fused Prtp (Prtp-GST), GST-fused Drpr (Drpr-GST), or GST alone, or were left untreated. The arrowheads point to the positions of Prtp (A) and Drpr (B).



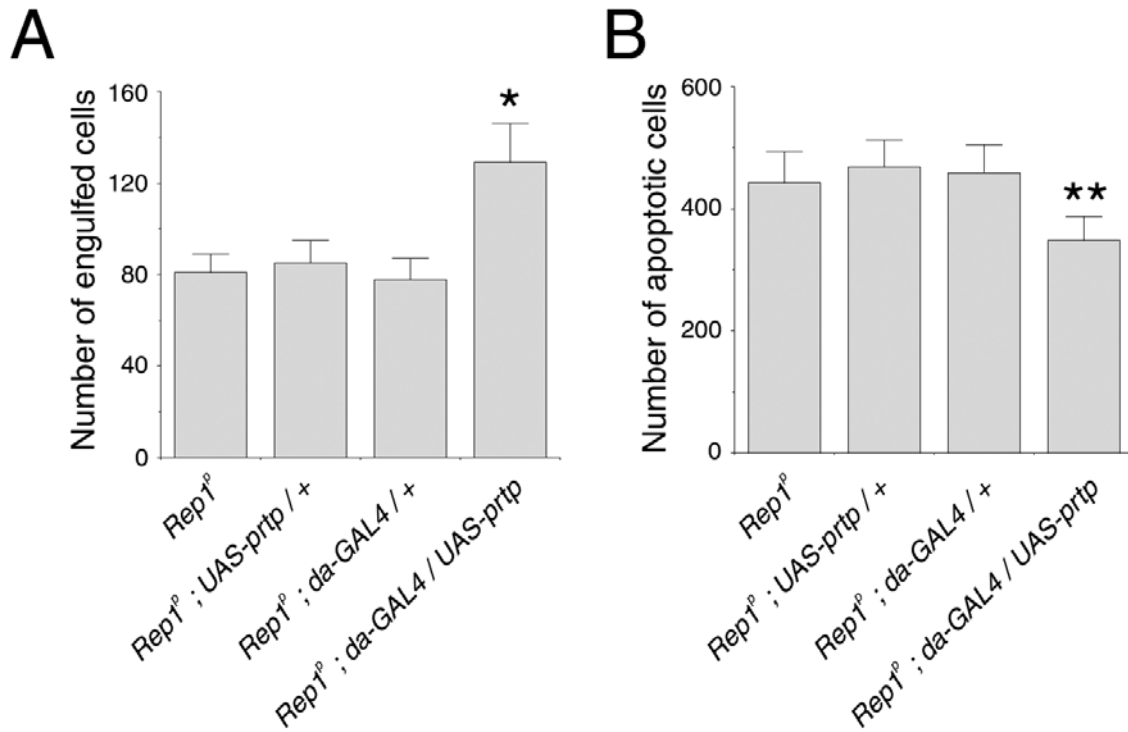
**Supplementary Figure S3** Characterization of *prtp* null mutants. (A) DNA of the indicated fly lines was analyzed by polymerase chain reaction (using primers shown with arrows in Figure 2A), and the amplified DNA was electrophoresed on an agarose gel followed by visualization with ethidium bromide. (B) Total RNA of adult flies of the indicated lines was subjected to reverse transcription-mediated polymerase chain reaction to determine the level of mRNA of Prtp and Drpr. (C) Lysates of adult flies of the indicated lines (*drpr<sup>A5</sup>* is a *drpr* null mutant) were analyzed for the level of Prtp and Drpr by Western blotting (70  $\mu$ g protein for Prtp and 140  $\mu$ g protein for Drpr). The arrows point to the corresponding positive signals.



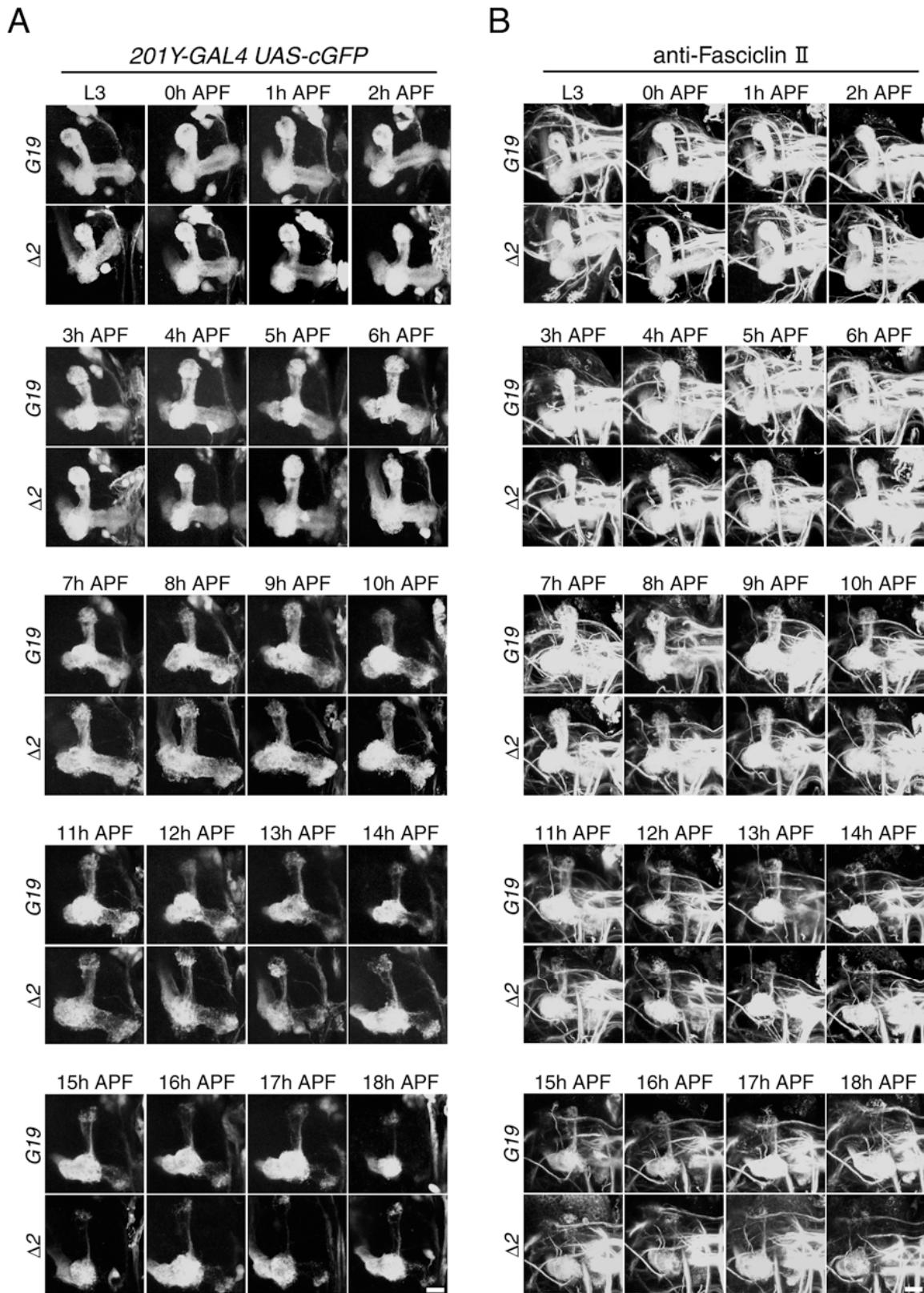
**Supplementary Figure S4** Occurrence of apoptosis during embryogenesis in the control (*prtp<sup>G19</sup>*) and *prtp* mutant (*prtp<sup>Δ1</sup>* and *prtp<sup>Δ2</sup>*) flies. Embryos at stages 10 and 11 of the indicated fly lines were histochemically analyzed for the presence of activated caspase (anti-activated caspase-3) and fragmented DNA (TUNEL). Positive signals in either assay are shown as dots located toward the anterior part of embryos. Bar, 0.1 mm.



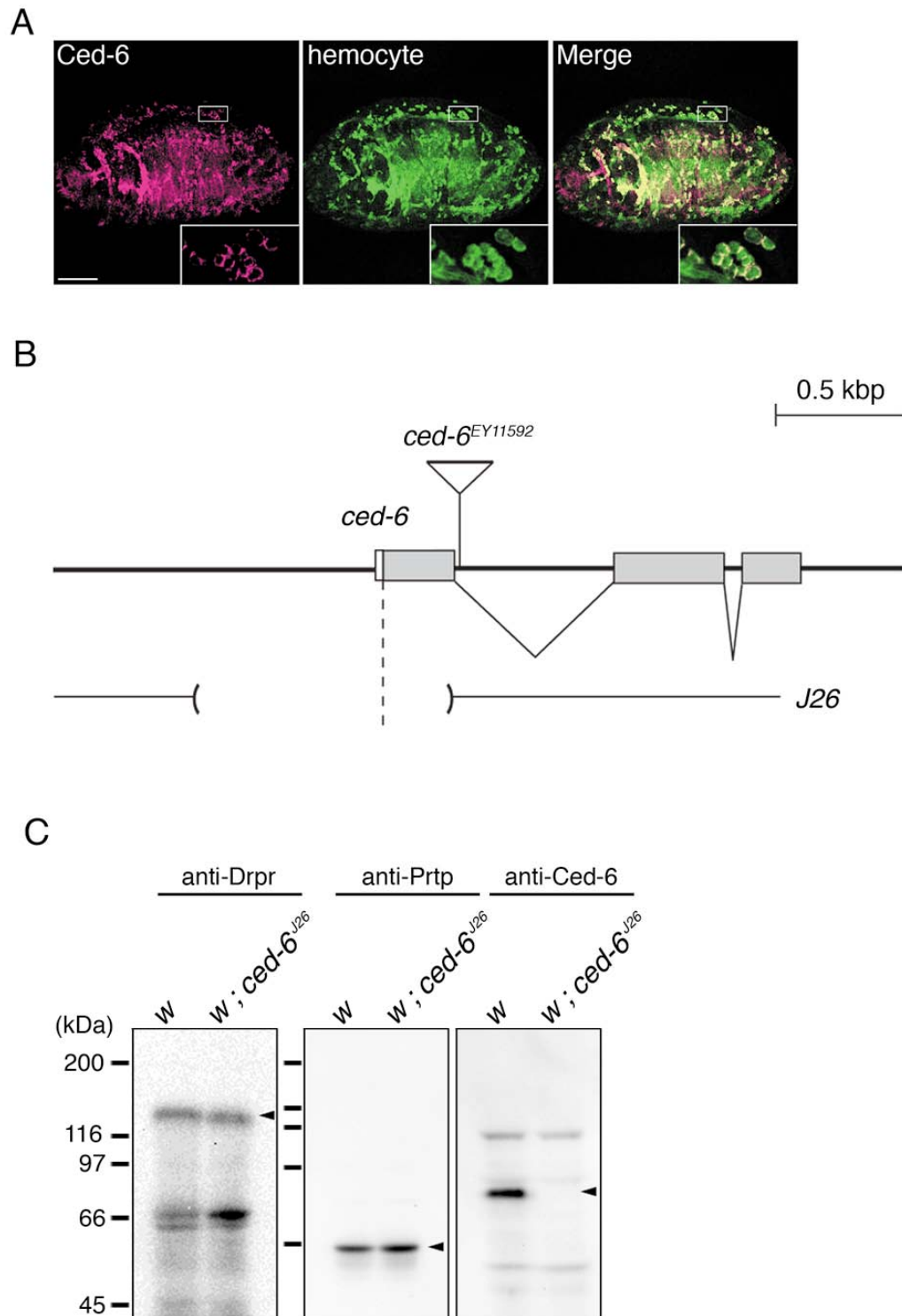
**Supplementary Figure S5** Identification of Croquemort-expressing hemocytes that have phagocytosed apoptotic cells in *Drosophila* embryos. Stage 16 embryos of  $w^{1118}$  flies were analyzed for the presence of hemocytes by immunohistochemistry with anti-Croquemort antibody (seen in blue) and of apoptotic cells by TUNEL (seen in brown). The inset is a magnified view of the squared area, and the arrowhead points to a Croquemort-positive hemocyte containing a TUNEL-positive nucleus. Bar, 10  $\mu\text{m}$ .



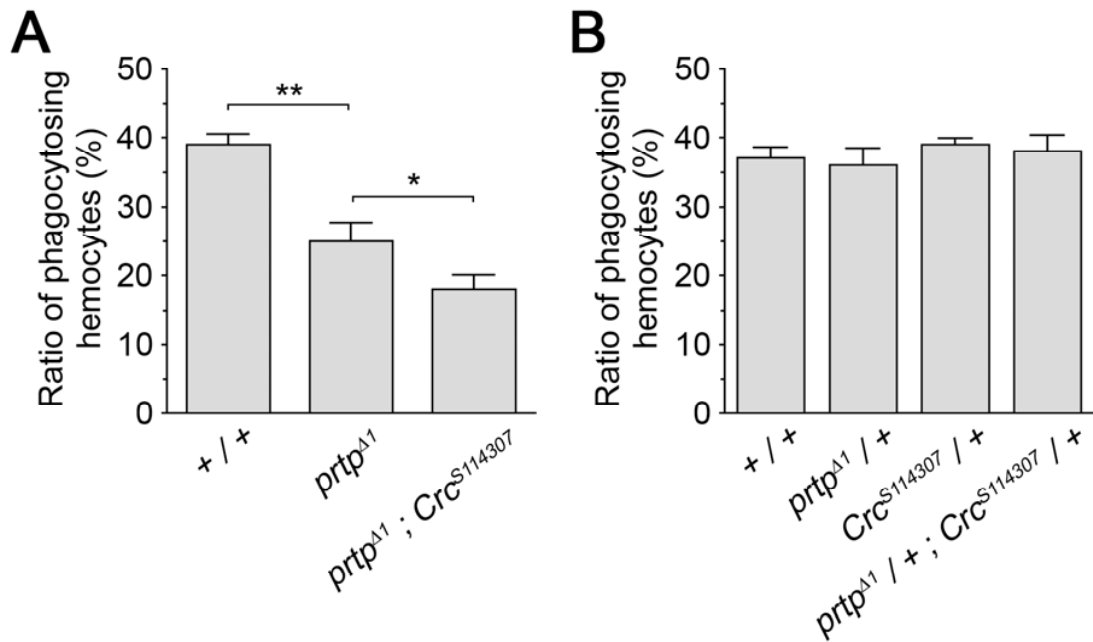
**Supplementary Figure S6** Increased level of phagocytosis and reduced number of apoptotic cells in embryos of *prtp*-overexpressing flies. The levels of phagocytosis (**A**) and apoptosis (**B**) in embryos of the indicated fly lines were determined by ISNT and staining with 7-amino actinomycin D (Franc *et al*, 1999), respectively. Data from one of 2 independent experiments that yielded similar results are shown as the mean ± s.d. \* $P < 0.001$  and \*\* $P < 0.01$ , compared with *Rep1<sup>p</sup>*;  $n = 10$  (A) and 5 (B) (number of embryos examined).



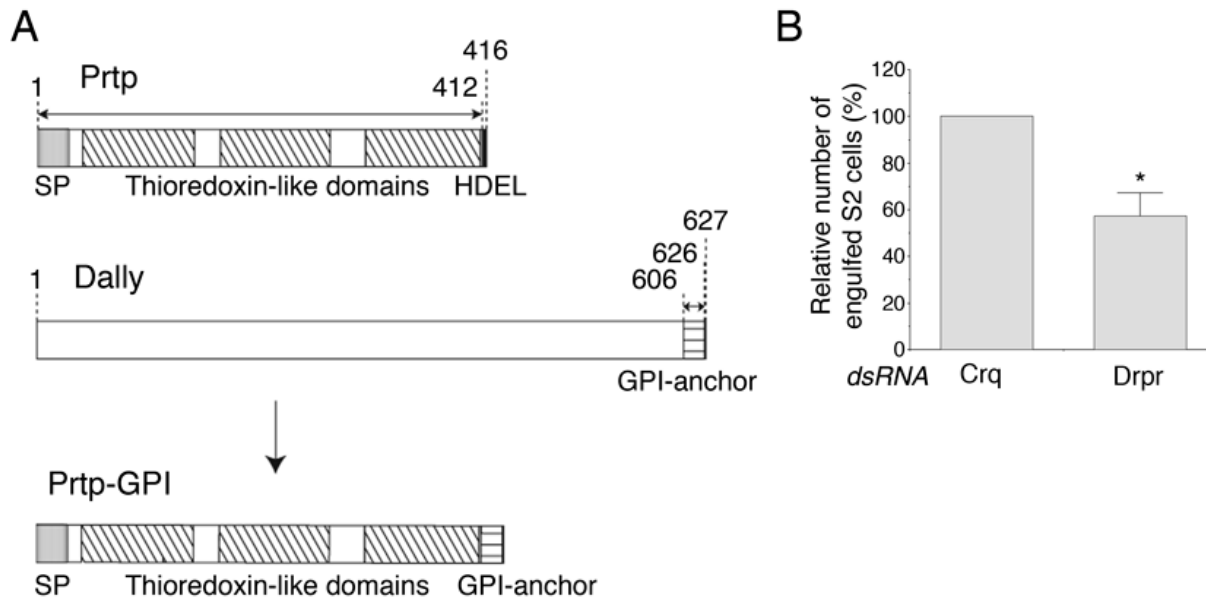
**Supplementary Figure S7** Normal pruning of  $\gamma$  neuron axons in *prtp* null mutant. The removal of  $\gamma$  neuron axons of larval mushroom bodies during metamorphosis was examined with the fly lines *prtp*<sup>G19</sup> (G19) and *prtp* <sup>$\Delta 2$</sup>  ( $\Delta 2$ ). Brains dissected from flies at the indicated developmental stages (L3, late third instar; APF, after puparium formation) were examined under a confocal laser-scanning microscope for the existence of  $\gamma$  neuron axons, which were visualized by histochemically detecting either GFP (forcedly expressed in a  $\gamma$  neuron-specific manner) (A) or Fasciclin II (specifically expressed in  $\alpha/\beta$  and  $\gamma$  neurons and immunochemically visualized) (B). Genotypes of the fly lines analyzed are: *w*<sup>1118</sup> *prtp*<sup>G19</sup> / Y ; *201Y-GAL4 UAS-cGFP* / + (G19), *w*<sup>1118</sup> *prtp* <sup>$\Delta 2$</sup>  / Y ; *201Y-GAL4 UAS-cGFP* / + ( $\Delta 2$ ). Bars, 20  $\mu$ m.



**Supplementary Figure S8** Generation of *ced-6* null mutant by P-element excision. **(A)** Expression of Ced-6 in hemocytes of *Drosophila* embryos. Stage 16 embryos of *srpHemo-GAL4 UAS-srcEGFP* flies (GFP was forcedly expressed in a hemocyte-specific manner) were immunohistochemically analyzed with anti-Ced-6 and anti-GFP (hemocyte) antibodies. The insets are magnified views of the corresponding squared areas. Bar, 100  $\mu$ m. **(B)** Schematic presentation of a portion of the *Drosophila* genome near *ced-6* of *ced-6*<sup>EY11592</sup> and *ced-6*<sup>J26</sup> (*J26*). The symbols are the same as those used in Figure 2A. The removal of the P-element caused a deletion in the region between nucleotide positions -697 and +295 (with the first nucleotide of the translation start codon of Ced-6 numbered +1, indicated by the dashed line). **(C)** Western blotting of lysates of adult flies of *w*<sup>1118</sup> and *ced-6*<sup>J26</sup> with anti-Drpr, anti-Prtp, and anti-Ced-6 antibodies (90  $\mu$ g protein for Drpr, 23  $\mu$ g protein for Prtp, and 45  $\mu$ g protein for Ced-6). The arrowheads point to the corresponding positive signals.



**Supplementary Figure S9** Relationship between *prtp* and *calreticulin* in the phagocytosis of apoptotic cells. Phagocytosis by hemocytes was examined with cells dispersed from embryos of the indicated fly lines (flies used as control (+ / +) were *prtp*<sup>G19</sup>). **(A)** The level of phagocytosis was compared between the *prtp* null mutant (*prtp*<sup>Δ1</sup>) and a double mutant for *prtp* and *calreticulin* (*prtp*<sup>Δ1</sup>; *Crc*<sup>S114307</sup>): *Crc*<sup>S114307</sup> is a null allele for *calreticulin*. \**P* < 0.02 and \*\**P* < 0.001. **(B)** To examine a genetic interaction between *prtp* and *calreticulin*, flies heterozygous for *prtp*<sup>Δ1</sup> (*prtp*<sup>Δ1</sup> / +), heterozygous for *Crc*<sup>S114307</sup> (*Crc*<sup>S114307</sup> / +), and *trans*-heterozygous for *prtp*<sup>Δ1</sup> and *Crc*<sup>S114307</sup> (*prtp*<sup>Δ1</sup> / + ; *Crc*<sup>S114307</sup> / +) were analyzed.



**Supplementary Figure S10** Construction of plasmid for the expression of glycosylphosphatidylinositol (GPI)-anchored Prtp and phagocytosis of S2 cells expressing Prtp-GPI. **(A)** cDNAs for Prtp and Dally were manipulated so that the amino acid residues 1–412 of Prtp, which contains the signal peptide (SP) but lacks the ER retention motif (HDEL), were linked with the amino acid residues 606–626, a site for GPI anchor attachment, of Dally. The resultant DNA was inserted into the vector pUAST and introduced into S2 cells. **(B)** S2 cells expressing Prtp-GPI were subjected to phagocytosis by l(2)mbn cells, which had been transfected with double-stranded RNA (*dsRNA*) containing a sequence of mRNA for Croquemort (Crq) or Drpr. The number of engulfed S2 cells was shown relative to that in the experiment with l(2)mbn cells transfected with double-stranded RNA containing a sequence of Crq mRNA.  $P < 0.001$ .